

THESIS APPROVED BY

4/8/19

Date



Stephen M. Gross, Ph.D., Chair



Mark A. Latta, D.M.D., M.S.



Barbara J. O'Kane, Ph.D., M.S.



Mark D. Markam, D.D.S



Gail M. Jensen, Ph.D., Dean

FLEXURAL STRENGTH AND FRACTURE TOUGHNESS OF FLOWABLE
COMPOSITES CONTAINING LOW STRESS MONOMERS AND
MICROCAPSULES

By

JOSHUA COUILLARD

A THESIS

Submitted to the faculty of the Graduate School of Creighton University in partial fulfillment of the requirements for the degree of Masters of Science in the Department of Oral Biology

Omaha, NE

April 08, 2019

ABSTRACT

The annual failure rates of composite restorations are low, though most of these failures are due to recurrent caries, fractures of the tooth structure or restorative materials. Volumetric shrinkage has received significant attention because of the role it plays in recurrent decay. In this study, low stress formulations were designed with the ability to release ions through the use of microcapsule technology to combat the causes of recurrent decay. To meet the recommendations of the Scientific Committee on Emerging and Newly Identified Health Risks, the formulations were also designed to be Bis-GMA free. This study examines the flexural strength and fracture toughness of these formulations and explores the effects of different variables on these mechanical properties. The variables include: the type of low stress monomer in the continuous phase, the UDMA/TEGMA ratio within the continuous phase, the amount of glass loaded, the amount of fumed silica loaded, and the inclusion of low viscosity monomers. The study confirms that these variables affect the flexural strength and fracture toughness of the formulations and suggest that there is potential for developing a low stress, BPA free, ion eluting flowable composite/ base liner.

ACKNOWLEDGEMENTS

I would like to thank Creighton University School of Dentistry and Dr. Neil Norton for the opportunity to contribute to research in the field of dentistry through this program. I am truly grateful for the time, knowledge, and support provided by Dr. Stephen Gross during both the research and writing processes of this thesis. I would like to thank Dr. Mark Latta for ensuring that the research was possible with the experience and resources provided. I also would like to thank Valeria Morales for her effort working alongside me every day. Finally, I would like to recognize Ben Kruse and Justin Pfeifer who contributed greatly to this project. I would like to express my gratitude to all of these individuals for making this thesis possible.

TABLE OF CONTENTS

ABSTRACT.....	v
ACKNOWLEDGEMENTS.....	vi
FIGURES AND TABLES	vii
CHAPTER 1: INTRODUCTION.....	1
1.1 Demineralization and remineralization of enamel	2
1.2 Restorations.	2
1.3 Recurrent caries	3
1.4 Low stress monomers.....	3
1.5 BPA byproduct release	5
1.6 Mechanical properties	6
1.7 Formulations.....	7
CHAPTER 2: MATERIALS & METHODS.....	8
2.1 Pre-polymer synthesis.....	9
2.2 Preparation of oil solution and salt solution.....	10
2.3 Microcapsule synthesis.....	10
2.4 Flowable composite formulations.....	11
2.5 Flexural strength testing	15
2.6 Fracture toughness testing.....	15
2.7 Statistical analysis.....	16
CHAPTER 3: RESULTS.....	17
3.1 Results.....	18

3.2	Low stress monomers	18
3.2.1	Varied low stress monomers	18
3.2.2	Constant LSM with different glass and fumed silica loading.....	28
3.3	Low viscosity monomers	36
3.3.1	Varied low stress monomers	36
3.3.2	Low viscosity monomers	48
3.3.3	Fumed silica	54
CHAPTER 4: DISCUSSION.....		63
4.1	Discussion.....	64
4.2	Low stress monomers.....	64
4.2.1	Varied low stress monomers.....	64
4.2.2	Constant LSM with different glass and fumed silica loading....	67
4.3	Low viscosity monomers.....	68
4.3.1	Varied low stress monomers.....	68
4.3.2	Low viscosity monomers.....	70
4.3.3	Fumed silica.....	71
4.4	Conclusion.....	72
REFERENCES.....		74

FIGURES AND TABLES

Figure 1.....5

Figure 2.....6

Table 1.....11

Table 2.....12

Table 3.....12

Table 4.....12

Table 5.....13

Table 6.....14

Figure 3a.....19

Figure 3b.....19

Figure 4a.....21

Figure 4b.....21

Figure 5a.....23

Figure 5b.....23

Figure 6a.....25

Figure 6b.....25

Figure 7a.....27

Figure 7b.....27

Figure 8a.....29

Figure 8b.....29

Figure 9a.....31

Figure 9b.....31

Figure 10a.....	33
Figure 10b.....	33
Figure 11a.....	35
Figure 11b.....	35
Figure 12a.....	37
Figure 12b.....	37
Figure 13a.....	39
Figure 13b.....	39
Figure 14a.....	41
Figure 14b.....	41
Figure 15a.....	43
Figure 15b.....	43
Figure 16a.....	45
Figure 16b.....	45
Figure 17a.....	47
Figure 17b.....	47
Figure 18a.....	49
Figure 18b.....	49
Figure 19a.....	51
Figure 19b.....	51
Figure 20a.....	53
Figure 20b.....	53
Figure 21a.....	55

Figure 21b.....	55
Figure 22a.....	57
Figure 22b.....	57
Figure 23a.....	59
Figure 23b.....	59
Figure 24a.....	61
Figure 24b.....	61

Chapter 1

Introduction

1.1 Demineralization and remineralization of enamel

Within the oral cavity the crystalline structures that make up the enamel of the human tooth undergo the process of demineralization by being chemically broken down through the removal of minerals, such as calcium and phosphate, from the hard surface. Remineralization counteracts the process by providing calcium, phosphate and fluoride to the tooth [1]. Demineralization occurs when there is an increase in the acidity within the oral environment. When the acid-producing bacteria found in dental plaque feed on fermentable carbohydrates, they produce organic acids (lactic and acetic) as by-products. If the pH reaches 5.5 or below, the acid that leaches into the tooth surface dissolves the carbonated hydroxyapatite in the tooth enamel, releasing calcium and phosphate [2]. Remineralization can occur naturally but can be aided by increasing the fluoride in the saliva. Saliva is crucial in the remineralization process because it naturally contains calcium, phosphate and fluoride enabling it to return minerals lost in the demineralization process while also neutralizing the acid, raising the pH in the oral cavity [3,4]. The fluoride in saliva is important to this process because it combines with the demineralized carbonated hydroxyapatite to form a fluorapatite layer [5-7]. In this layer, the fluoride replaces the hydroxide, creating a sturdier coating for the enamel with greater resistance to acid dissolution. Tooth decay occurs when the rate of demineralization is greater than the rate of remineralization in the tooth surface [8].

1.2 Restorations

If the demineralization leads to cavitation and loss of tooth structure a dental restoration will become necessary. The purpose of placing dental restorations is to remove the decay and fill the cavity to restore the integrity and functionality of the tooth

[9]. To accomplish this, the tooth is prepared by cutting out any decay and weakened or unsupported tooth structure. Once the tooth is prepared a direct restoration, a restoration placed within the mouth by building up the missing tooth structure, or an indirect restoration, a restoration created outside the mouth and placed at a later time, is placed to repair the missing tooth structure. Dental restorations can be created from a variety of materials including metals and metal alloys, glass ionomer cements, porcelain, or composite resins [10]. Because of the ability to color match with the tooth and the longevity of restorations, composite resins have become increasingly popular [11-18].

1.3 Recurrent caries

Although composite restorations have low annual failure rates, most are due to recurrent caries or fractures of the tooth structure or restorative materials [16-18]. Recurrent caries, or secondary caries, is decay found beneath a previously placed dental restoration. Recurrent caries can occur for a few different reasons. If the decay was not completely removed during the preparation process prior to filling the cavity, the existing decay can continue to spread. Additionally, recurrent decay can occur if a margin is left between the restoration and the tooth. This can be due to the margins not being completely sealed when placing the restoration, the restoration breaking down near the margin, or the volumetric shrinkage of the restoration pulling it away from the tooth surface [19-24].

1.4 Low stress monomers

Because of the role it plays in recurrent decay, volumetric shrinkage has received significant attention in recent years. The volumetric shrinkage for dimethacrylate-based materials is around 2–4% [25]. Stress is generated at the interface between the composite

and cavity wall because the adhesion to the cavity wall restricts the volumetric shrinkage of the composite [26,27]. This can lead to fractures in the tooth structure, fractures in the composite, or a separation of the two along the adhesive layer [28-31]. Shrinkage is linked to the degree of polymerization [32]. As the degree of conversion of the monomers increases, the composite shrinks as a result of the decreasing van der Waal radii between monomers as covalent bonds form between individual molecules [33]. Additionally, as the filler load increases in a formulation, the total volumetric shrinkage decreases [34,35].

To minimize the volumetric shrinkage, clinical strategies such as filling the tooth cavity in increments or curing with low initial irradiance have been attempted. In addition to the clinical strategies, attempts have been made to develop new materials designed to minimize volumetric shrinkage [29,30]. The different chemical approaches used to address volumetric shrinkage include: the use of monomers with lower molar shrinkage coefficients, the creation of higher molecular weight oligomers for use in the continuous phase, or the addition of pre-polymerized additives [29,36,37]. Terathane oligomers and thiourethane oligomers have higher molecular weight than standard monomers used in most continuous phases (e.g. Bis-GMA, UDMA, or TEGMA). For Terathanes, the polytetrahydrofuran (Fig. 1) segment comprises a significant amount of the molecular weight and provides rotational freedom within the molecule. In addition to high molecular weight, the thiourethane monomer has thiol functional groups which work as a chain transfer agent to reduce the rate of polymerization of methacrylates in an attempt to decrease the stress development in the polymer network [38-41].

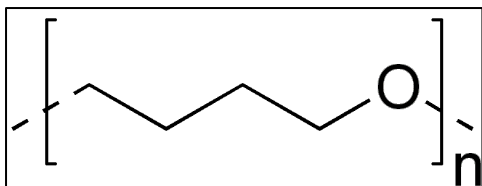


Figure 1. Chemical structure of polytetrahydrofuran. For Terathane 650, n averages 9 and for Terathane 1000, n averages 14.

1.5 BPA byproduct release

Bisphenol A (BPA) is an organic synthetic substance with two hydroxyphenyl functional groups and a dimethylmethylen group (Fig. 2). This substance, which has been found to be harmful to humans and animals, is commonly used in the production of polycarbonate plastics and epoxy resins used in many industries including dentistry [42,43]. Previous studies have shown that BPA is an endocrine disruptor, causing multiple negative effects on various internal organs and systems. This is primarily due to its similarity to estrogen and its ability to act on estrogen receptors [44,45]. BPA has been found to affect the hormonal, cardiovascular and digestive systems. High exposure to BPA can even increase the possibility of cancer, diabetes, hypertension, atherosclerosis and many other diseases [46]. Bis-GMA may release BPA byproducts. It has been found that after the placement of Bis-GMA composites, children and adolescents had an increase in BPA concentrations in their urine for the first two weeks. After that period, an increase in urinary BPA concentration was not detected. This suggests that BPA byproducts may leach from recently placed composite restorations [43].

The Scientific Committee on Emerging and Newly Identified Health Risks (SCENIHR) in Europe reported that long-term exposure to dental materials containing BPA derivatives was below the BPA temporary value for tolerable daily intake (t-TDI) set by the European Food Safety Authority (EFSA). Additionally, the report recommends

that BPA free medical and dental materials are preferable, and that the replacement of BPA should be considered [47].

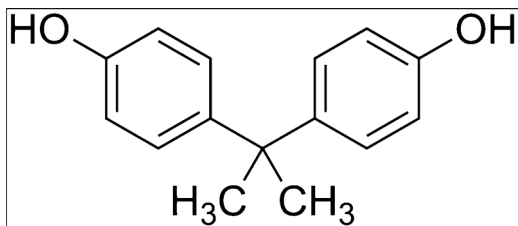


Figure 2. Chemical structure of the BPA.

1.6 Mechanical properties

In the oral environment, restorative materials are exposed to mechanical challenges. Testing the mechanical properties of flexural strength and fracture toughness are particularly important when determining the durability and potential for success of a flowable composite. Stress is the ability of a material to resist an external load applied to the material with a value equal to the force per unit area. Flexural strength of a material is the force per unit area at the instant of fracture when the specimen undergoes flexural loading. Flexural strength must be determined by bending multiple specimens of the same shape and size at the same rate [48]. Flexural strength is crucial for testing dental restorations because the occlusal points of contact have forces acting on small areas causing bending stress in restorations [49]. Fractures or flaws can occur in a material causing weakened areas. To prevent failure of restorations, it is essential to ensure that the composite has a high fracture toughness. Fracture toughness is the mechanical property that describes a materials resistance to the propagation of flaws under an applied stress [48].

1.7 Formulations

In this study, the formulations were designed to be low stress, ion releasing, Bis-

GMA free, light initiated flowable composites/ base liners. To help combat demineralization and secondary caries, the flowable composites made contained low stress monomers and microcapsules to release calcium, phosphate, and fluoride ions to assist in remineralization. These ion permeable microcapsules have demonstrated that they can be incorporated into resin composites and have a slow, controlled release of ions [50-52]. The following four low stress monomers (LSM) were compared: Terathane 650 extended urethane methacrylate (650 Meth), Terathane 1000 extended urethane methacrylate (1000 Meth), Terathane 650 extended urethane acrylate (650 Acr), and a thiourethane oligomer (TU). UDMA was used instead of Bis-GMA in each of the formulations in this study to limit the release of BPA byproducts. A range of formulations were created examining the effect of the ratio of UDMA/TEGMA within the continuous phase, the type of low stress monomer, the amount of glass, the amount of fumed silica, and the type of low viscosity monomer (LVM), on the flexural strength and fracture toughness in the presence of microcapsules.

Chapter 2

Materials and Methods

2.1 Pre-polymer synthesis

A polyurethane pre-polymer was synthesized by a solution polymerization in cyclohexanone (Sigma Aldrich). For this study, polyurethane was synthesized using isophorone-diisocyanate (Fluka) and ethylene glycol (Sigma Aldrich). First, a flask was evacuated and flame dried. Then, nitrogen gas was gradually introduced to the flask. While allowing the inert gas to continue to flow through the flow adapter, cyclohexanone was added. Next, the isophorone-diisocyanate was added using a syringe. The septum was replaced and secured. A syringe needle was inserted through the septum, to relieve pressure inside the flask, while the solution stirred. After stirring for 30 minutes, ethylene glycol and an initiator were added. The septum was replaced a final time and secured. Next, the flask was carefully lowered into an oil bath. A degassing needle, connected to the manifold, was inserted until it rested at the bottom of the flask. Then the adjacent inert gas port on the manifold (connecting to the hose of the degassing needle) was opened slowly until the reaction mixture began to bubble. Once complete, the solution degassed at room temperature for 30 minutes. Once complete, the degassing needle was removed and the reaction mixture was set to 70°C. Once the temperature was set, the reaction ran overnight.

On day two, the flask was removed from the oil bath and cooled for one hour. After, the solution was transferred, fitted to a flow adapter, and secured to a vacuum line from a cold trap. The dewar was filled approximately one third of the way with isopropanol (Fisher Scientific). Dry ice was added to the dewar in small pieces while the cold trap was in place. Following this, the round bottom flask was lowered into the oil

bath, and set to 100°C. All exposed glassware including the cold trap, flow adapter, and round bottom flask were insulated.

The flask was then evacuated, so that the evaporating solvent could travel into the trap and liquefy in a cold environment. The vacuum was pulled until the pre-polymer appeared dry and all of the solvent was recovered from the product. The pre-polymer was then collected and stored in vials in a cabinet at room temperature until microcapsule synthesis.

2.2 Preparation of oil solution and salt solution

The preparatory solutions were made at least 24 hours prior to microcapsule synthesis. The oil solution consisted of methyl benzoate (Acros), an emulsifying agent, and the polyurethane pre-polymer. The three components were combined in an Erlenmeyer flask and stirred until the polyurethane was dispersed.

The salt solutions were made to accommodate our desired molarity for ion release. For this experiment, we used 3.0 M potassium phosphate dibasic (Fisher Scientific), 5.0 M calcium nitrate tetrahydrate (Alfa Aesar) and 0.8 M sodium fluoride (MP Biomedicals) solutions. It is important to note that the higher concentrations were given a significant amount of time to dissolve, in some cases, overnight. Solutions were stored at room temperature until use.

2.3 Microcapsule synthesis

The prepared pre-polymer oil solution was agitated to create a reverse emulsion and the aqueous salt solution was then added incrementally over a period of fifteen minutes while the oil solution was agitated in a reactor at 70 °C. The polyurethane was then chain extended using ethylene glycol to create the desired product. The

microcapsules were then centrifuged and stored for use in the flowable composite formulations.

2.4 Flowable composite formulations

The formulations in this study were prepared to be a low stress, ion releasing, Bis-GMA free, light initiated flowable composites. The formulations consisted of w/w% loadings of monomers UDMA and TEGMA (Esstech), Terathanes (DM Healthcare Products), thiourethane, HEMA or HPMA (DM Healthcare Products), glass (Schott), fumed silica (Evonik), photoinitiator (MP Biomedicals), and microcapsules. The flowable composites were prepared with loadings of 5 w/w% microcapsules containing 0.8 M sodium fluoride (MP Biomedicals), 5.0 M calcium nitrate tetrahydrate (Alfa Aesar), and 3.0 M potassium phosphate dibasic (Fisher Scientific) aqueous salt solutions.

ID Number	Glass	Fumed Silica	Continuous Phase Ratio (UDMA/TEGMA/Terathane)
1A	55	2.5	30/50/20
2A	55	2.5	40/40/20
3A	55	3.0	40/40/20
4A	60	2.5	30/50/20
5A	63	2.5	30/50/20

Table 1. The formulations of flowable composites where the ratio of Terathane 650 extended urethane methacrylate in the continuous phase and microcapsules were held constant. The loading of glass, fumed silica and UDMA/TEGMA ratios varied. All values are given in w/w%.

ID Number	Glass	Fumed Silica	Continuous Phase Ratio (UDMA/TEGMA/Terathane)
1B	55	2.5	30/50/20
2B	55	2.5	40/40/20
3B	60	2.5	30/50/20
4B	60	3.0	30/50/20
5B	63	2.5	30/50/20

Table 2. The formulations of flowable composites where the ratio of Terathane 1000 extended urethane methacrylate in the continuous phase and microcapsules were held constant. The loading of glass, fumed silica and UDMA/TEGMA ratios varied. All values are given in w/w%.

ID Number	Glass	Fumed Silica	Continuous Phase Ratio (UDMA/TEGMA/Terathane)
1C	55	2.5	30/50/20
2C	55	2.5	40/40/20
3C	55	3.0	40/40/20
4C	60	2.5	30/50/20
5C	63	2.5	30/50/20

Table 3. The formulations of flowable composites where the ratio of Terathane 650 extended urethane acrylate in the continuous phase and microcapsules were held constant. The loading of glass, fumed silica and UDMA/TEGMA ratios varied. All values are given in w/w%.

ID Number	Glass	Fumed Silica	Continuous Phase Ratio (UDMA/TEGMA/Thiourethane)
1D	50	2.5	40/40/20
2D	50	3.0	40/40/20
3D	55	2.5	40/40/20
4D	55	3.0	40/40/20
5D	60	2.5	30/50/20
6D	60	3.0	30/50/20
7D	60	2.5	40/40/20
8D	60	3.0	40/40/20

Table 4. The formulations of flowable composites where the ratio of thiourethane in the continuous phase and microcapsules were held constant. The loading of glass, fumed silica and UDMA/TEGMA ratios varied. All values are given in w/w%.

ID Number	Glass	Fumed Silica	Continuous Phase Ratio (UDMA/TEGMA/Terathane/LVM)	Low Viscosity Monomer	Low Stress Monomer
1E	60	2.5	40/38/20/2	HEMA	650 Meth
2E	60	2.5	40/38/20/2	HPMA	650 Meth
3E	60	2.5	40/38/20/2	HEMA	650 Acr
4E	60	2.5	40/38/20/2	HPMA	650 Acr
5E	63	2.5	30/48/20/2	HEMA	1000 Meth
6E	63	2.5	30/48/20/2	HPMA	1000 Meth
7E	63	2.5	40/38/20/2	HEMA	1000 Meth
8E	63	2.5	40/38/20/2	HPMA	1000 Meth
9E	60	2.5	40/35/20/5	HEMA	650 Meth
10E	60	2.5	40/35/20/5	HPMA	650 Meth
11E	60	2.5	40/35/20/5	HEMA	650 Acr
12E	60	2.5	40/35/20/5	HPMA	650 Acr
13E	63	2.5	30/45/20/5	HEMA	1000 Meth
14E	63	2.5	30/45/20/5	HPMA	1000 Meth
15E	60	2.5	40/30/20/10	HEMA	650 Meth
16E	60	2.5	40/30/20/10	HPMA	650 Meth
17E	60	2.5	40/30/20/10	HEMA	650 Acr
18E	60	2.5	40/30/20/10	HPMA	650 Acr
19E	63	2.5	30/40/20/10	HEMA	1000 Meth
20E	63	2.5	30/40/20/10	HPMA	1000 Meth

Table 5. The formulations of flowable composites where the ratio of Terathane in the continuous phase and microcapsules were held constant. The loading of glass, fumed silica and UDMA/TEGMA/LVM ratios as well as the type of low stress monomer and low viscosity monomer varied. All values are given in w/w%.

ID Number	Glass	Fumed Silica	Continuous Phase Ratio (UDMA/TEGMA/LSM)	Low Stress Monomer
1F	60	2.0	40/40/20	TU
2F	60	2.0	40/40/20	650 Meth
3F	60	2.0	40/40/20	1000 meth
4F	60	2.0	40/40/20	650 Acr
5F	60	2.5	30/50/20	TU
6F	60	2.5	30/50/20	650 Meth
7F	60	2.5	30/50/20	1000 Meth
8F	60	2.5	30/50/20	650 Acr
9F	60	2.5	40/40/20	TU
10F	60	2.5	40/40/20	650 Meth
11F	60	2.5	40/40/20	1000 Meth
12F	60	2.5	40/40/20	650 Acr
13F	60	3.0	40/40/20	TU
14F	60	3.0	40/40/20	650 Meth
15F	60	3.0	40/40/20	1000 Meth
16F	60	3.0	40/40/20	650 Acr

Table 6. The formulations of flowable composites where the ratio of low stress monomer in the continuous phase and w/w% of 10-MDP and microcapsules were held constant. Each formulation contains 1% 10-MDP. The loading of glass, fumed silica and UDMA/TEGMA ratios as well as the type of low stress monomer varied. All values are given in w/w%.

2.5 Flexural strength testing

A 3-point flexural test was performing using 10 bend bar specimens (2×2×25mm) made according to the dimensions specified by ISO 4049/2000 [53]. The specimens were prepared by compressing the restorative material between two glass plates, separated by a Teflon mold. Irradiation occurred on top and bottom of the specimens for 90 s using an Optilux 501 halogen curing light unit (Kerr), followed by 5 minutes in a Triad 2000 light curing oven (Densply), which assured that the whole surface was cured. After removal from the mold, the specimens were polished with 600 grit sand paper in order to get rid of disturbing edges or bulges. All specimens were then stored an oven at 40°C prior to testing for a minimum of 7 days. Intact bar specimens without any defects or chipped edges were adjusted to a 3-point flexural test using a supporting span of 20 mm. The 3-point flexural strength was determined at a crosshead speed of 1.0 mm/min (n = 10) using the universal testing machine (MTS Insight Electromechanical – 1 kN standard length). The 3-point flexural strength (σ) was calculated using the following equation: $\sigma = 3Fl/2bh^2$, where F is the maximum stress determined by the universal testing machine (MTS Insight Electromechanical – 1 kN standard length), and l, b, and h are the span length, width, and height of the specimen, respectively [54].

2.6 Fracture toughness testing

The fracture toughness (K_{IC}) was determined using ten single-edge notched-beam specimens of each material. The specimens (25 mm length × 5 mm height × 2.5 mm width) were made by compressing the restorative material between two glass plates, separated by a steel mold with a razor blade fragment inserted to create a 2 mm deep notch. The width of the notch was determined by the thickness of

the blade. Irradiation occurred on top and bottom of the specimens for 90 s using an Optilux 501 halogen curing light unit (Kerr), followed by 5 minutes in a Triad 2000 light curing oven (Densply), which assured that the whole surface was cured. After removal from the mold, the specimens were polished with 600 grit sand paper in order to get rid of disturbing edges or bulges. All specimens were then stored in an oven at 40°C prior to testing for a minimum of 7 days. Intact bar specimens without any defects or chipped edges were adjusted to a fracture toughness test using a supporting span (L) of 20 mm. The samples were loaded until failure in a universal testing machine (MTS Insight Electromechanical – 1 kN standard length). During testing, the crosshead speed was 1.0 mm/min. The universal testing machine measured the force during bending as a function of deflection of the beam. Load-deflection (P = load) curves were recorded; the height (B) and the width (W) of the specimens were measured with a micrometer and the notch depth (a) was calculated by measuring the lip with a micrometer and subtracting it from the height. K_{IC} was calculated from measurements with the single-edge notched-beam specimens as [55,56]:

$$K_{IC} = \frac{3PL}{2BW^2} \left\{ 1.93 \left(\frac{a}{W} \right)^{\frac{1}{2}} - 3.07 \left(\frac{a}{W} \right)^{\frac{3}{2}} + 14.53 \left(\frac{a}{W} \right)^{\frac{5}{2}} - 25.11 \left(\frac{a}{W} \right)^{\frac{7}{2}} + 25.8 \left(\frac{a}{W} \right)^{\frac{9}{2}} \right\}$$

2.7 Statistical analysis

The average value for flexural strength and fracture toughness were determined for each of the samples after removing the outliers. Outliers were identified with a 95% certainty using the Grubbs' test for outliers. The Tukey method was used to compare the sample values to determine if any samples had a statistically different flexural strength or fracture toughness. All samples that were found to be statistically different from one another were found with a 95% certainty.

Chapter 3

Results

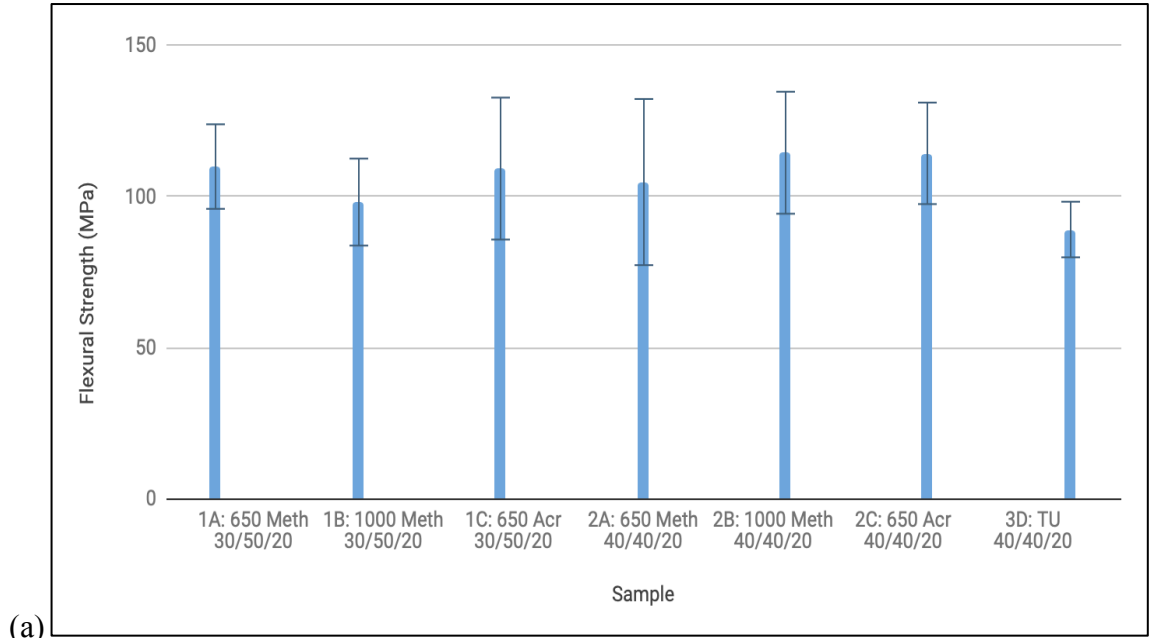
3.1 Results

In this study, the flexural strength and fracture toughness were determined for a number of formulations designed to be low stress, ion releasing, Bis-GMA free, light initiated flowable composites. To compare the effects of the materials used within the, a variety of formulations were created with the amount of low stress monomer and microcapsules held constant. The variables within the variety of formulations include: the type of low stress monomer in the continuous phase, the UDMA/TEGMA ratio within the continuous phase, the amount of glass loaded, the amount of fumed silica loaded, and the inclusion of low viscosity monomers. The average value for flexural strength and fracture toughness were determined after identifying outliers using the Grubbs' test for outliers.

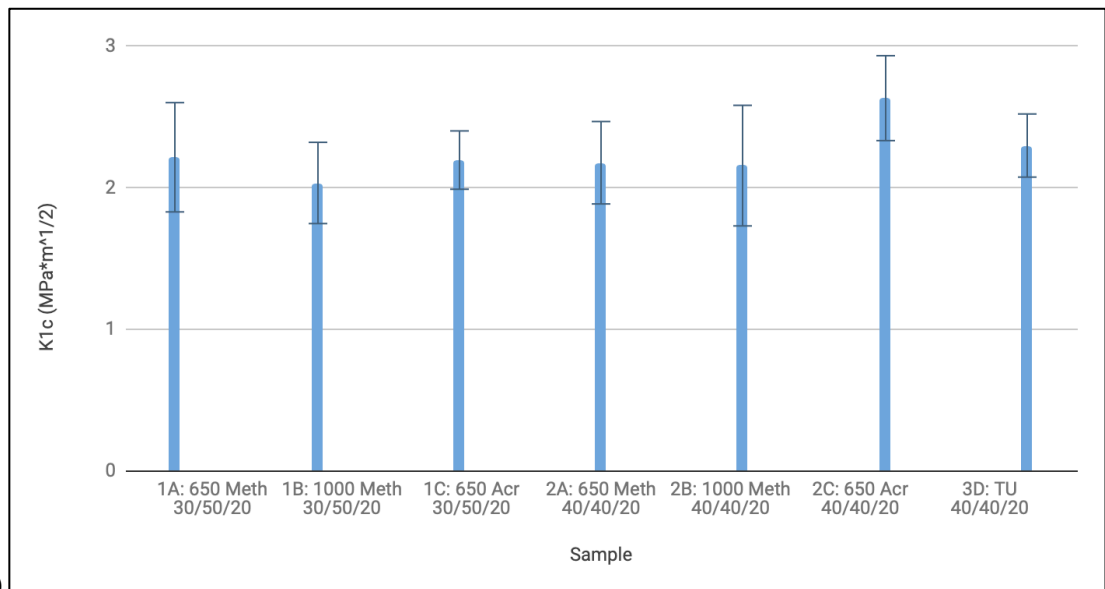
3.2 Low stress monomers

3.2.1 Varied low stress monomers

To examine the effect of the different low stress monomers on flexural strength and fracture toughness, the following graphs compare formulations where the type of low stress monomers differed while the amount of glass and fumed silica were held constant. Figures 3- 7 illustrate the effect the different low stress monomers have on the flexural strength and fracture toughness in several different formulations.



(a)



(b)

Figure 3. In Figure (a) the flexural strength; and Figure (b) the fracture toughness of formulations where the chemical identity of four different low stress monomers was changed in the continuous phase of each formulation. Each formulation was loaded with 55 w/w% glass, 2.5 w/w% fumed silica, 5 w/w% microcapsules and a continuous phase ratio of UDMA/TEGMA/LSM of either 30/50/20 or 40/40/20.

In Figure 3 (a) the flexural strength; and Figure 3 (b) the fracture toughness of formulations where the chemical identity of four different low stress monomers was changed in the continuous phase of each formulation. Each formulation was loaded with 55 w/w% glass, 2.5 w/w% fumed silica, 5 w/w% microcapsules and a continuous phase ratio of UDMA/TEGMA/LSM of either 30/50/20 or 40/40/20. For flexural strength, the following averages and standard deviations (in MPa) were determined for the various formulations: 109.93 ± 14.0 (1A: 650 Meth 30/50/20), 98.17 ± 14.4 (1B: 1000 Meth 30/50/20), 109.26 ± 23.5 (1C: 650 Acr 30/50/20), 104.8 ± 27.5 (2A: 650 Meth 40/40/20), 114.51 ± 20.2 (2B: 1000 Meth 40/40/20), 114.31 ± 16.8 (2C: 650 Acr 40/40/20), and 89.09 ± 9.2 (3D: TU 40/40/20). For fracture toughness, the following K_{IC} averages and standard deviations (in $\text{MPa} \cdot \text{m}^{1/2}$) were determined for the various formulations: 2.21 ± 0.386 (1A: 650 Meth 30/50/20), 2.03 ± 0.287 (1B: 1000 Meth 30/50/20), 2.19 ± 0.206 (1C: 650 Acr 30/50/20), 2.18 ± 0.291 (2A: 650 Meth 40/40/20), 2.16 ± 0.426 (2B: 1000 Meth 40/40/20), 2.63 ± 0.3 (2C: 650 Acr 40/40/20), and 2.3 ± 0.223 (3D: TU 40/40/20).

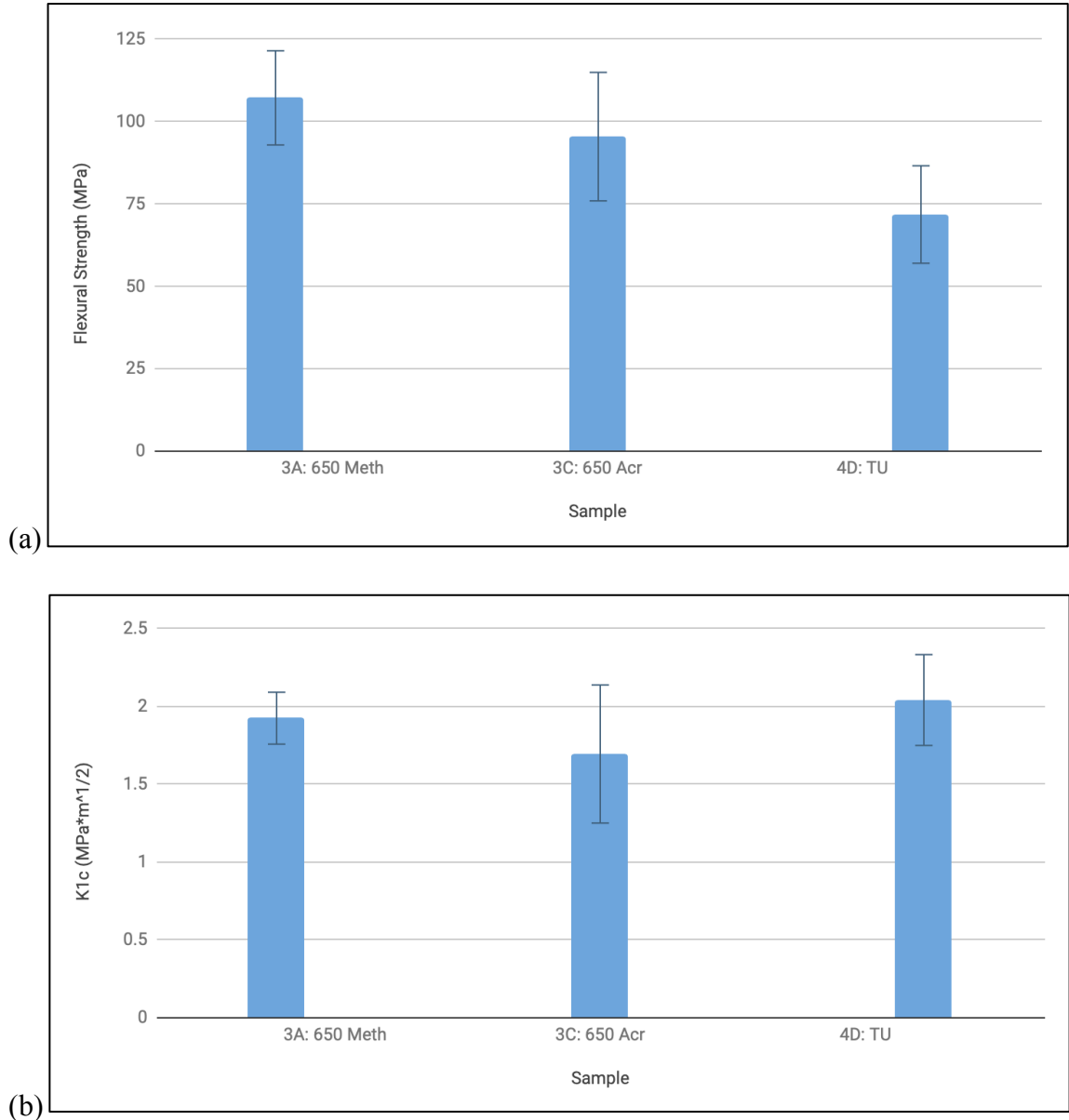
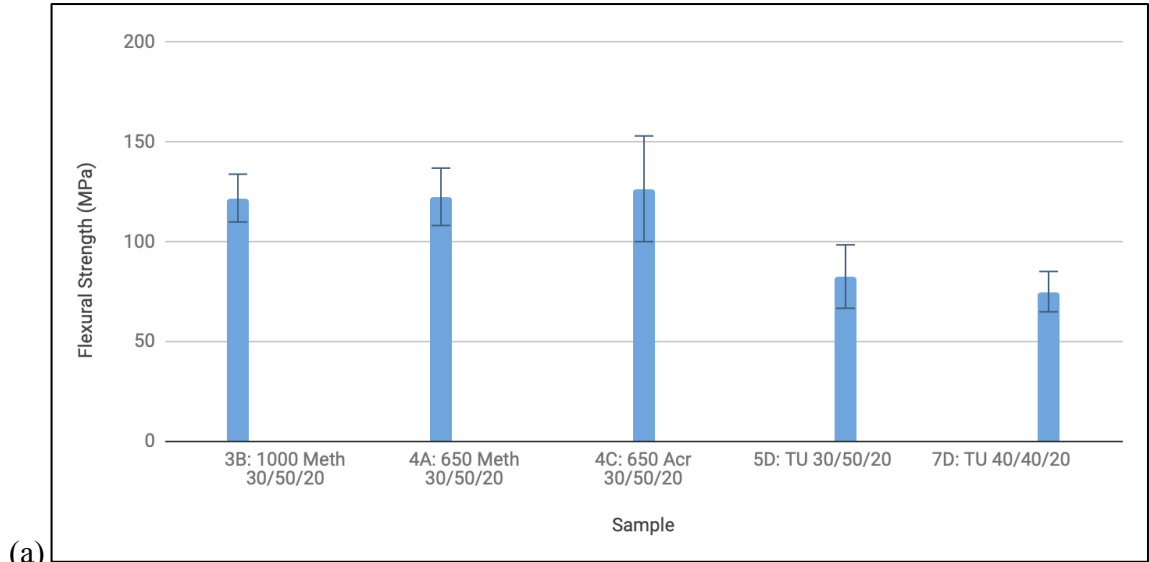
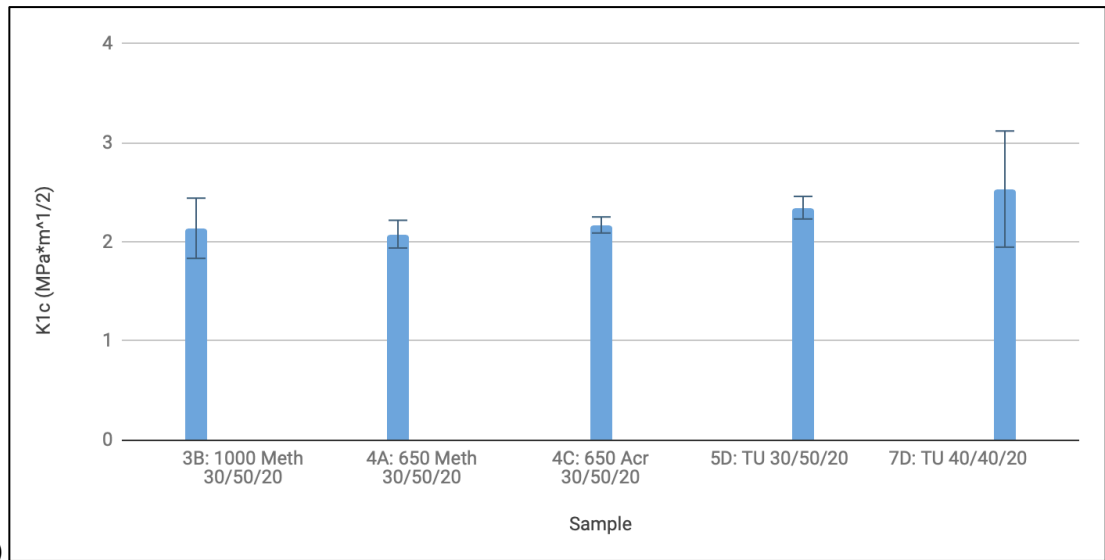


Figure 4. In Figure (a) the flexural strength; and Figure (b) the fracture toughness of formulations where the chemical identity of three different low stress monomers was changed in the continuous phase of each formulation. Each formulation was loaded with 55 w/w% glass, 3.0 w/w% fumed silica, 5 w/w% microcapsules and a continuous phase ratio of UDMA/TEGMA/LSM of 40/40/20.

Figure 4 (a) and (b) differ from Figure 3 (a) and (b) by increasing fumed silica from 2.5 w/w% to 3.0 w/w% with a continuous phase ratio of UDMA/TEGMA/LSM of 40/40/20. For flexural strength, the following averages and standard deviations (in MPa) were determined for the various formulations: 107.16 ± 14.3 (3A: 650 Meth), 95.39 ± 19.5 (3C: 650 Acr), and 71.74 ± 14.8 (4D: TU). For fracture toughness, the following K_{IC} averages and standard deviations (in $\text{MPa} \cdot \text{m}^{1/2}$) were determined for the various formulations: 1.92 ± 0.167 (3A: 650 Meth), 1.69 ± 0.444 (3C: 650 Acr), and 2.04 ± 0.292 (4D: TU).



(a)



(b)

Figure 5. In Figure (a) the flexural strength; and Figure (b) the fracture toughness of formulations where the chemical identity of four different low stress monomers was changed in the continuous phase of each formulation. Each formulation was loaded with 60 w/w% glass, 2.5 w/w% fumed silica, 5 w/w% microcapsules and a continuous phase ratio of UDMA/TEGMA/LSM of either 30/50/20 or 40/40/20.

Figure 5 (a) and (b) differ from Figure 3 (a) and (b) by increasing glass load from 55 w/w% to 60% w/w%. For flexural strength, the following averages and standard deviations (in MPa) were determined for the various formulations: 121.83 ± 12.0 (3B: 1000 Meth 30/50/20), 122.47 ± 14.4 (4A: 650 Meth 30/50/20), 126.5 ± 26.5 (4C: 650 Acr 30/50/20), 82.48 ± 15.9 (5D: TU 30/50/20), and 74.91 ± 10.1 (7D: TU 40/40/20). For fracture toughness, the following K_{IC} averages and standard deviations (in $\text{MPa} \cdot \text{m}^{1/2}$) were determined for the various formulations: 2.14 ± 0.304 (3B: 1000 Meth 30/50/20), 2.08 ± 0.14 (4A: 650 Meth 30/50/20), 2.17 ± 0.081 (4C: 650 Acr 30/50/20), 2.34 ± 0.115 (5D: TU 40/40/20), and 2.53 ± 0.586 (7D: TU 40/40/20).

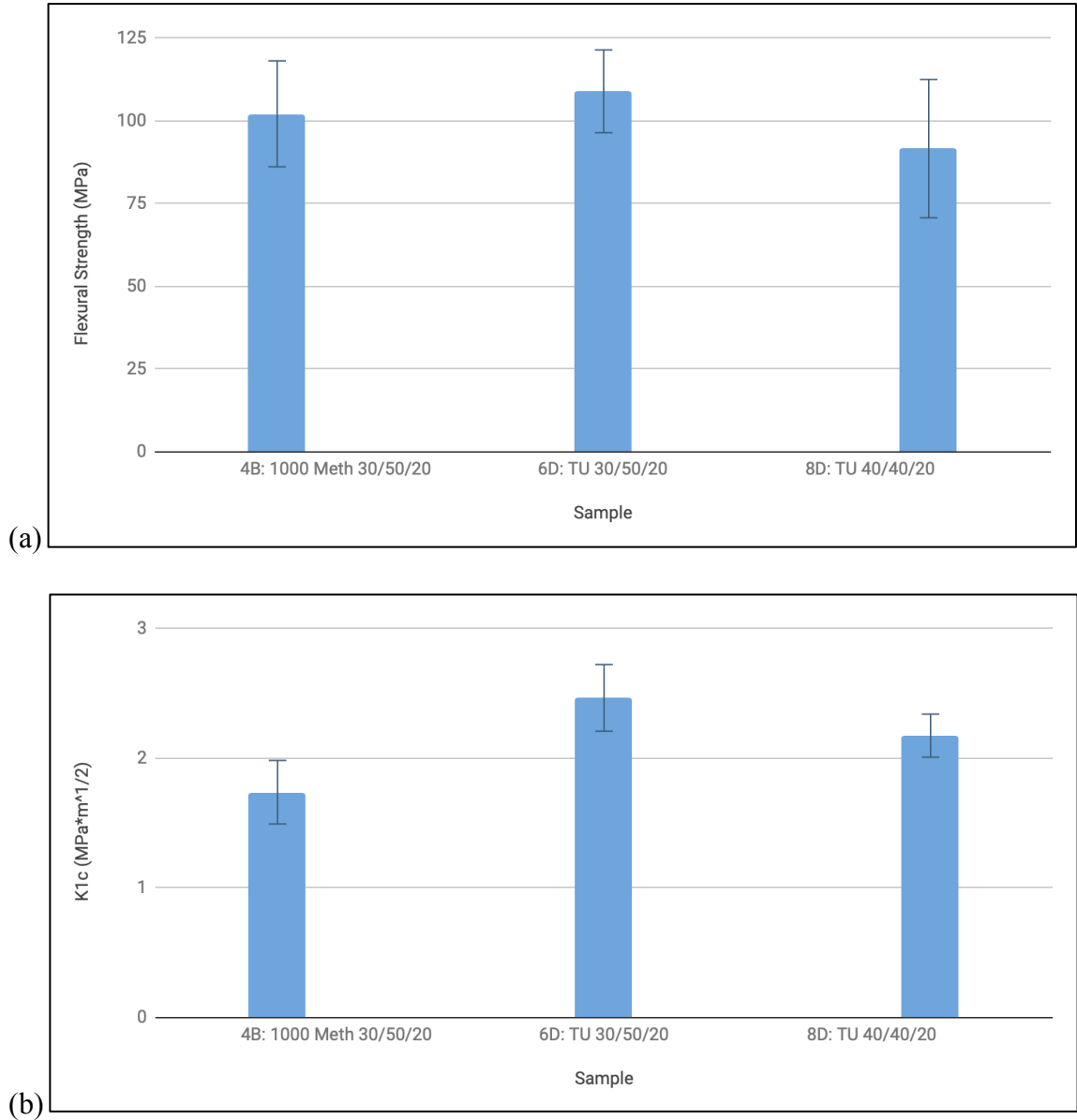


Figure 6. In Figure (a) the flexural strength; and Figure (b) the fracture toughness of formulations where the chemical identity of two different low stress monomers was changed in the continuous phase of each formulation. Each formulation was loaded with 60 w/w% glass, 3.0 w/w% fumed silica, 5 w/w% microcapsules and a continuous phase ratio of UDMA/TEGMA/LSM of either 30/50/20 or 40/40/20.

Figure 6 (a) and (b) differ from Figure 3 (a) and (b) by increased fumed silica from 2.5 w/w% to 3.0 w/w%, glass from 55 w/w% to 60 w/w%. For flexural strength, the following averages and standard deviations (in MPa) were determined for the various formulations: 102.07 ± 16.0 (4B: 1000 Meth), 108.88 ± 12.5 (6D: TU), and 91.56 ± 20.90 (8D: TU). For fracture toughness, the following K_{IC} averages and standard deviations (in $\text{MPa} \cdot \text{m}^{1/2}$) were determined for the various formulations: 1.74 ± 0.245 (4B: 1000 Meth), 2.46 ± 0.257 (6D: TU), and 2.17 ± 0.166 (8D: TU).

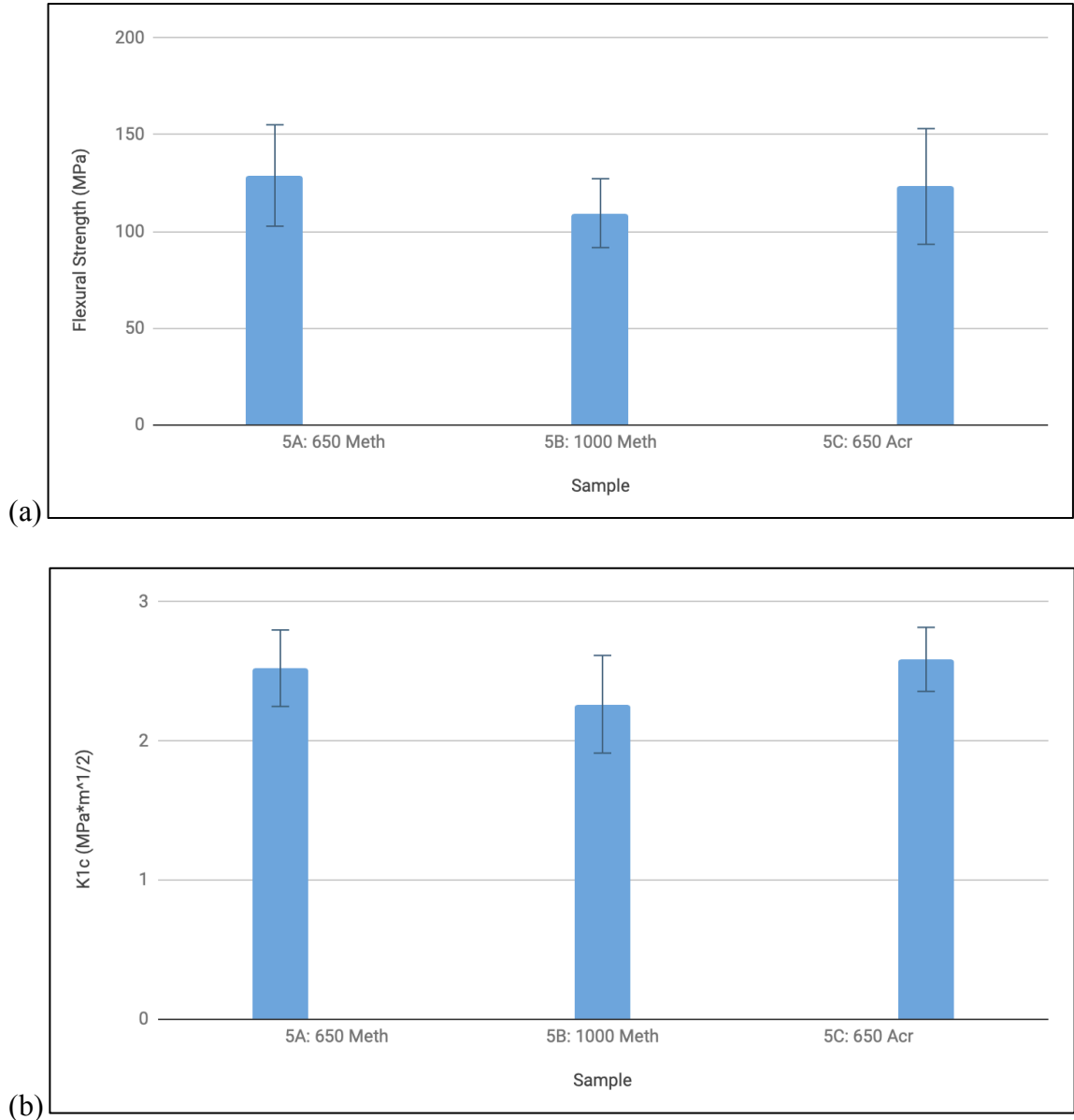


Figure 7. In Figure (a) the flexural strength; and Figure (b) the fracture toughness of formulations where the chemical identity of three different low stress monomers was changed in the continuous phase of each formulation. Each formulation was loaded with 63 w/w% glass, 2.5 w/w% fumed silica, 5 w/w% microcapsules and a continuous phase ratio of UDMA/TEGMA/LSM of 30/50/20.

Figure 7 (a) and (b) differ from Figure 3 (a) and (b) by increased glass from 55 w/w% to 63 w/w% glass with a continuous phase ratio of UDMA/TEGMA/LSM of 30/50/20. For flexural strength, the following averages and standard deviations (in MPa) were determined for the various formulations: 128.85 ± 26.2 (5A: 650 Meth), 109.39 ± 17.8 (5B: 1000 Meth), and 123.19 ± 29.9 (5C: 650 Acr). For fracture toughness, the following K_{IC} averages and standard deviations (in $\text{MPa} \cdot \text{m}^{1/2}$) were determined for the various formulations: 2.52 ± 0.275 (5A: 650 Meth), 2.26 ± 0.351 (5B: 1000 Meth), and 2.59 ± 0.23 (5C: 650 Acr).

3.2.2 Constant LSM with different glass and fumed silica loading

Figures 8-11 compare the effects of glass and fumed silica loading on flexural strength and fracture toughness for each low stress monomer formula created. Within the following graphs the glass loading, fumed silica loading, and continuous phase ratio were the variables that changed while the low stress monomer remained constant. Each figure in 8-11 depicts a different LSM with different glass and fumed silica loadings.

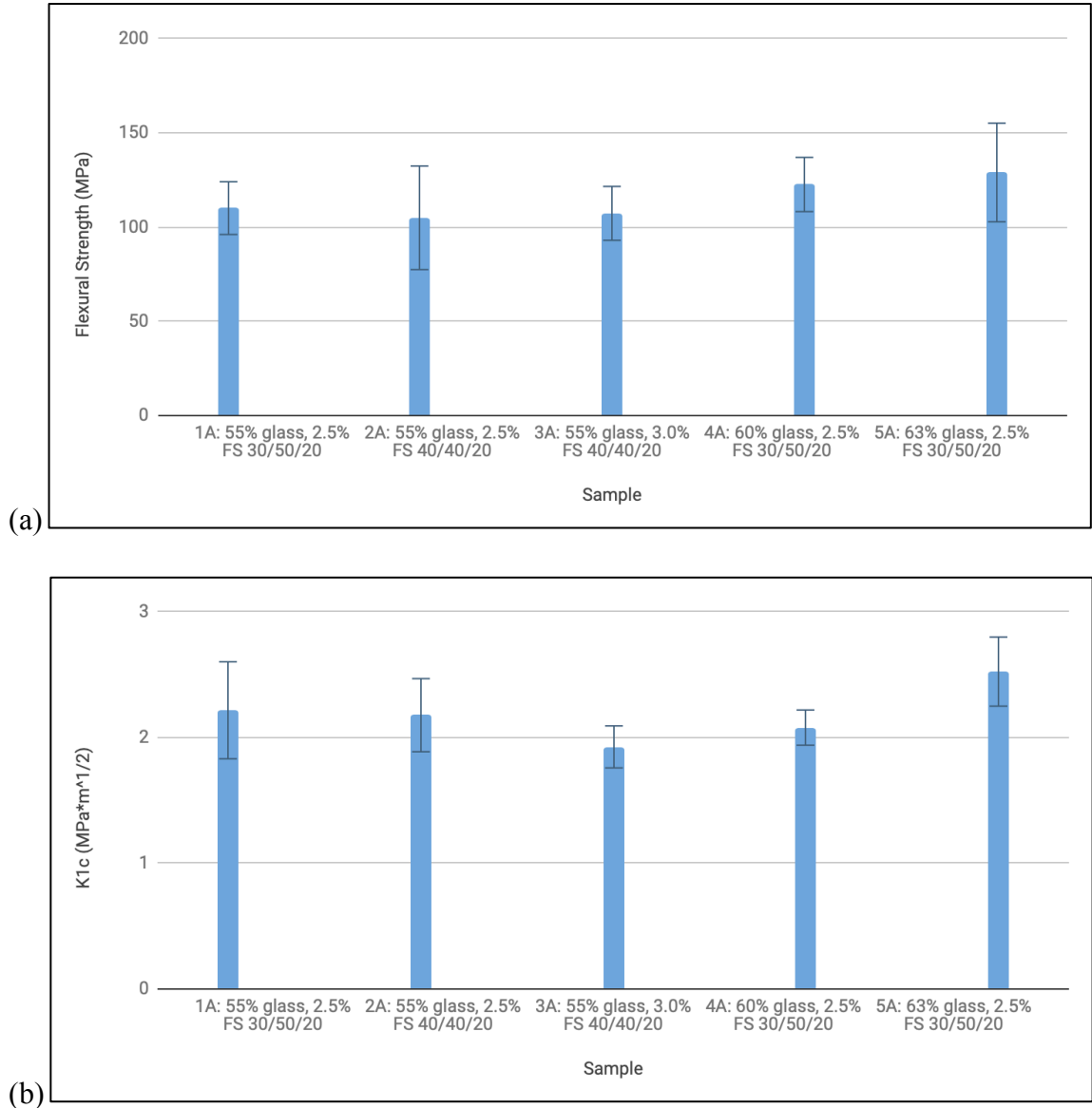


Figure 8. In Figure (a) the flexural strength; and Figure (b) the fracture toughness of formulations where each was created using Terathane 650 extended urethane methacrylate as the low stress monomer. Each formulation was loaded with 55, 60, or 63 w/w% glass, 2.5 or 3.0 w/w% fumed silica, 5 w/w% microcapsules and a continuous phase ratio of UDMA/TEGMA/LSM of either 30/50/20 or 40/40/20.

In Figure 8 (a) the flexural strength; and Figure 8 (b) the fracture toughness of formulations where each was created using Terathane 650 extended urethane methacrylate as the low stress monomer. Each formulation was loaded with 55, 60, or 63 w/w% glass, 2.5 or 3.0 w/w% fumed silica, 5 w/w% microcapsules and a continuous phase ratio of UDMA/TEGMA/LSM of either 30/50/20 or 40/40/20. For flexural strength, the following averages and standard deviations (in MPa) were determined for the various formulations: 109.93±14.0 (1A: 55% glass, 2.5% FS 30/50/20), 104.8±27.5 (2A: 55% glass, 2.5% FS 40/40/20), 107.16±14.3 (3A: 55% glass, 3.0% FS 40/40/20), 122.47±14.4 (4A: 60% glass, 2.5% FS 30/50/20), and 128.85±26.2 (5A: 63% glass, 2.5% FS 30/50/20). For fracture toughness, the following K_{IC} averages and standard deviations (in MPa*m^{1/2}) were determined for the various formulations: 2.21±0.386 (1A: 55% glass, 2.5% FS 30/50/20), 2.18±0.291 (2A: 55% glass, 2.5% FS 40/40/20), 1.92±0.167 (3A: 55% glass, 3.0% FS 40/40/20), 2.08±0.14 (4A: 60% glass, 2.5% FS 30/50/20), and 2.52±0.275 (5A: 63% glass, 2.5% FS 30/50/20).

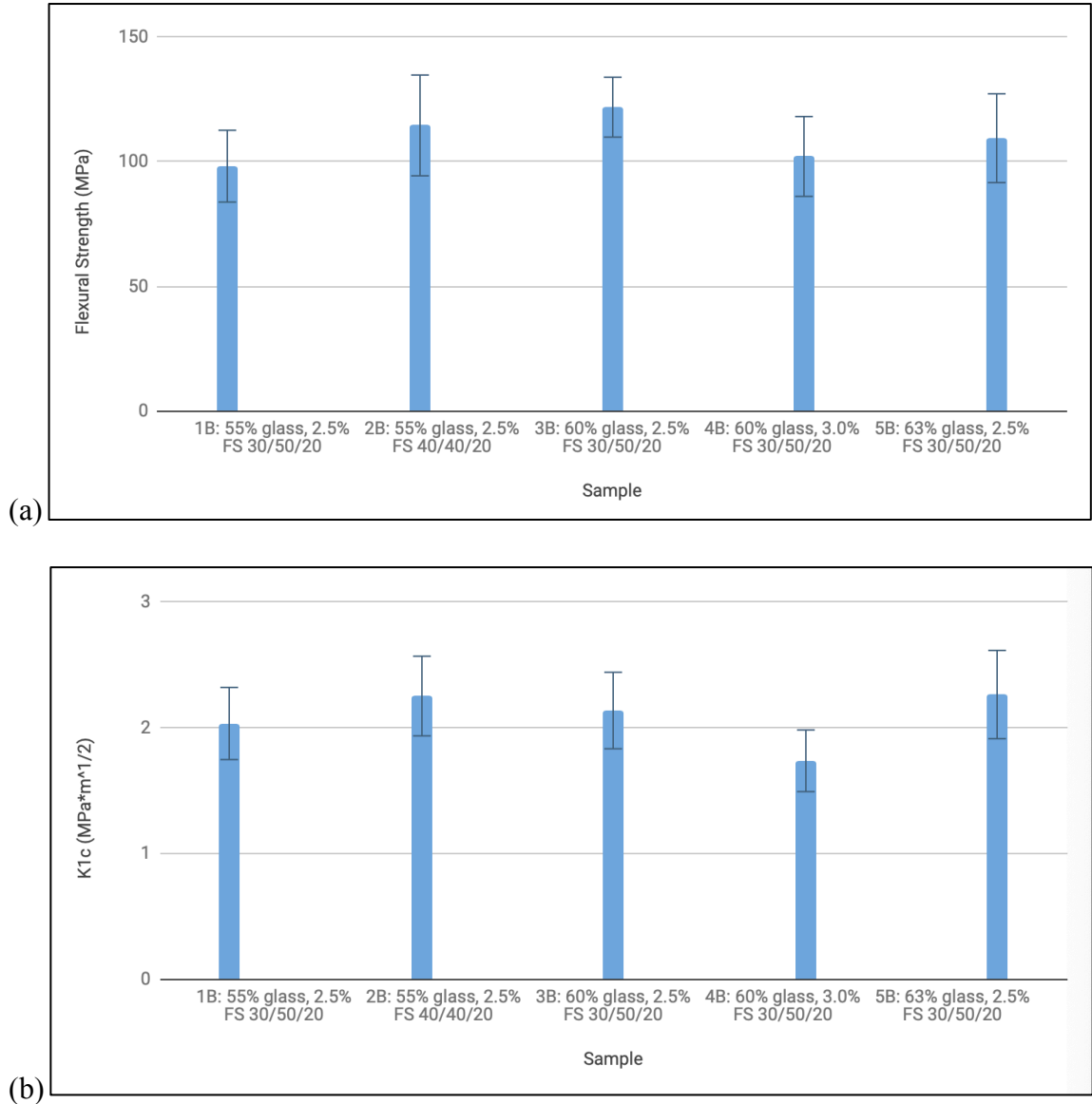


Figure 9. In Figure (a) the flexural strength; and Figure (b) the fracture toughness of formulations where each was created using Terathane 1000 extended urethane methacrylate as the low stress monomer. Each formulation was loaded with 55, 60, or 63 w/w% glass, 2.5 or 3.0 w/w% fumed silica, 5 w/w% microcapsules and a continuous phase ratio of UDMA/TEGMA/LSM of either 30/50/20 or 40/40/20.

Figure 9 (a) and (b) differ from Figure 8 (a) and (b) by changing 650 Meth with 1000 Meth. For flexural strength, the following averages and standard deviations (in MPa) were determined for the various formulations: 98.17 ± 14.4 (1B: 55% glass, 2.5% FS 30/50/20), 114.51 ± 20.2 (2B: 55% glass, 2.5% FS 40/40/20), 121.83 ± 12.0 (3B: 60% glass, 2.5% FS 30/50/20), 102.07 ± 16.0 (4B: 60% glass, 3.0% FS 30/50/20), and 109.39 ± 17.8 (5B: 63% glass, 2.5% FS 30/50/20). For fracture toughness, the following K_{IC} averages and standard deviations (in $\text{MPa} \cdot \text{m}^{1/2}$) were determined for the various formulations: 2.03 ± 0.287 (1B: 55% glass, 2.5% FS 30/50/20), 2.25 ± 0.317 (2B: 55% glass, 2.5% FS 40/40/20), 2.14 ± 0.304 (3B: 60% glass, 2.5% FS 30/50/20), 1.74 ± 0.245 (4B: 60% glass, 3.0% FS 30/50/20), and 2.26 ± 0.351 (5B: 63% glass, 2.5% FS 30/50/20).

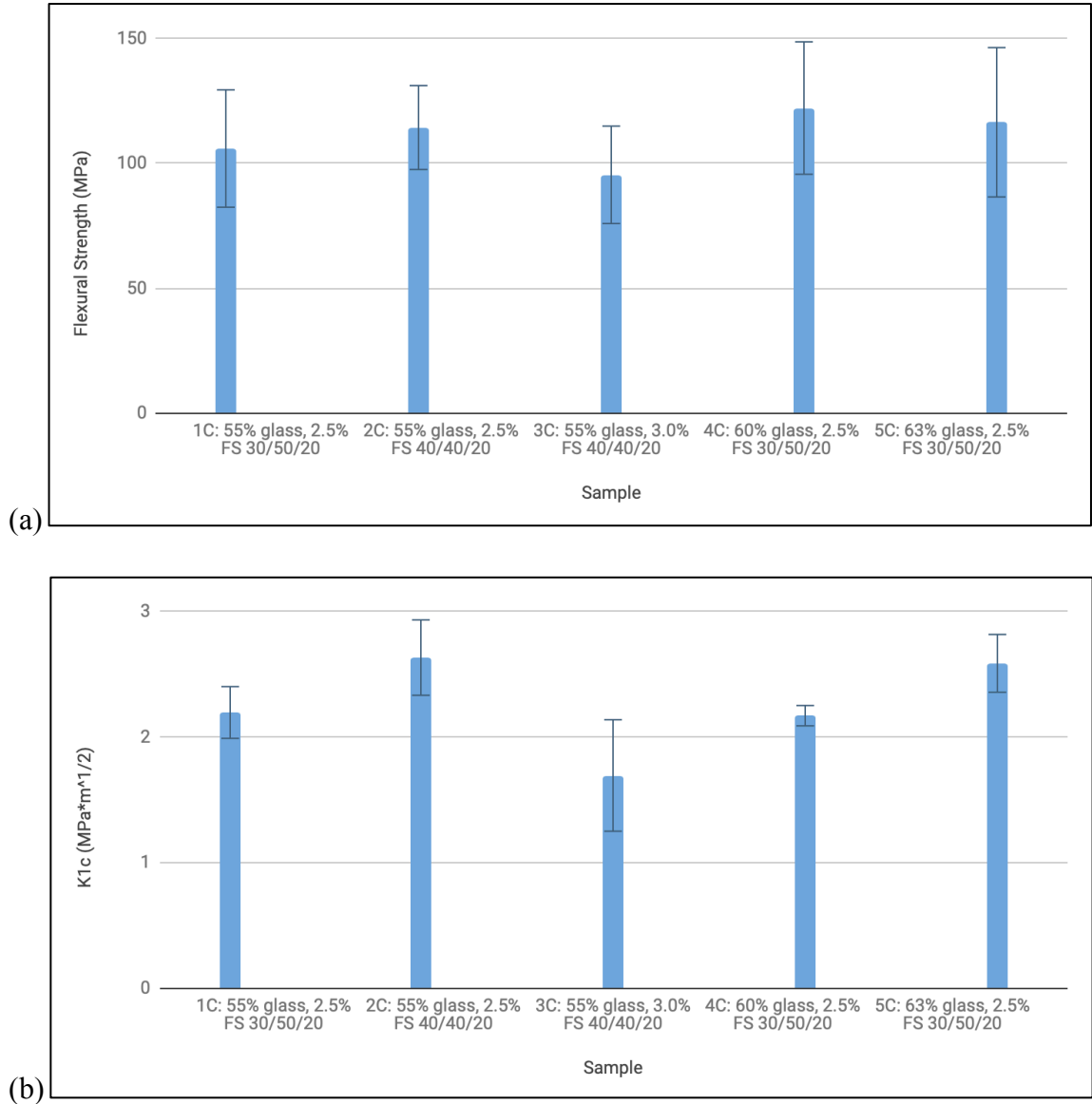


Figure 10. In Figure (a) the flexural strength; and Figure (b) the fracture toughness of formulations where each was created using Terathane 650 extended urethane acrylate as the low stress monomer. Each formulation was loaded with 55, 60, or 63 w/w% glass, 2.5 or 3.0 w/w% fumed silica, 5 w/w% microcapsules and a continuous phase ratio of UDMA/TEGMA/LSM of either 30/50/20 or 40/40/20.

Figure 10 (a) and (b) differ from Figure 8 (a) and (b) by changing 650 Meth with 650 Acr. For flexural strength, the following averages and standard deviations (in MPa) were determined for the various formulations: 105.92 ± 23.5 (1C: 55% glass, 2.5% FS 30/50/20), 114.31 ± 16.8 (2C: 55% glass, 2.5% FS 40/40/20), 95.39 ± 19.5 (3C: 55% glass, 3.0% FS 40/40/20), 122.13 ± 26.5 (4C: 60% glass, 2.5% FS 30/50/20), and 116.42 ± 29.9 (5C: 63% glass, 2.5% FS 30/50/20). For fracture toughness, the following K_{IC} averages and standard deviations (in $\text{MPa} \cdot \text{m}^{1/2}$) were determined for the various formulations: 2.19 ± 0.206 (1C: 55% glass, 2.5% FS 30/50/20), 2.63 ± 0.3 (2C: 55% glass, 2.5% FS 40/40/20), 1.69 ± 0.444 (3C: 55% glass, 3.0% FS 40/40/20), 2.17 ± 0.081 (4C: 60% glass, 2.5% FS 30/50/20), and 2.59 ± 0.23 (5C: 63% glass, 2.5% FS 30/50/20).

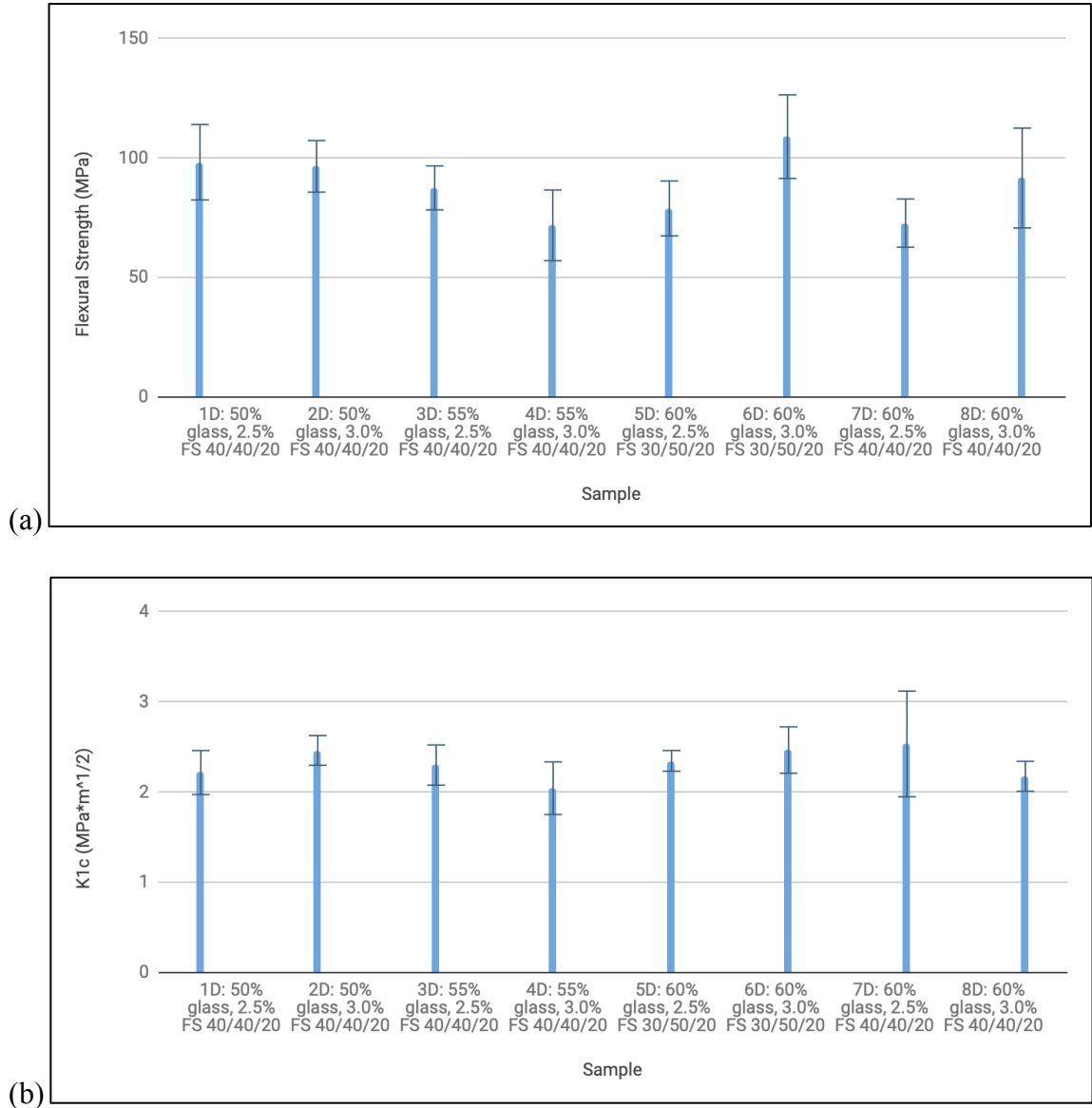


Figure 11. In Figure (a) the flexural strength; and Figure (b) the fracture toughness of formulations where each was created using the thiourethane oligomer as the low stress monomer. Each formulation was loaded with 50, 55, or 60 w/w% glass, 2.5 or 3.0 w/w% fumed silica, 5 w/w% microcapsules and a continuous phase ratio of UDMA/TEGMA/LSM of either 30/50/20 or 40/40/20.

Figure 11 (a) and (b) differ from Figure 8 (a) and (b) by changing 650 Meth with TU and including 50 w/w% glass instead of 63 w/w% glass. For flexural strength, the following averages and standard deviations (in MPa) were determined for the various formulations: 98.16 ± 15.8 (1D: 50% glass, 2.5% FS 40/40/20), 96.46 ± 10.8 (2D: 50% glass, 3.0% FS 40/40/20), 87.42 ± 9.2 (3D: 55% glass, 2.5% FS 40/40/20), 71.74 ± 14.8 (4D: 55% glass, 3.0% FS 40/40/20), 78.82 ± 11.5 (5D: 60% glass, 2.5% FS 30/50/20), 108.88 ± 17.5 (6D: 60% glass, 3.0% FS 30/50/20), 72.69 ± 10.1 (7D: 60% glass, 2.5% FS 40/40/20), and 91.56 ± 20.9 (8D: 60% glass, 3.0% FS 40/40/20). For fracture toughness, the following K_{IC} averages and standard deviations (in $\text{MPa} \cdot \text{m}^{1/2}$) were determined for the various formulations: 2.21 ± 0.244 (1D: 50% glass, 2.5% FS 40/40/20), 2.46 ± 0.165 (2D: 50% glass, 3.0% FS 40/40/20), 2.3 ± 0.223 (3D: 55% glass, 2.5% FS 40/40/20), 2.04 ± 0.292 (4D: 55% glass, 3.0% FS 40/40/20), 2.34 ± 0.115 (5D: 60% glass, 2.5% FS 30/50/20), 2.46 ± 0.257 (6D: 60% glass, 3.0% FS 30/50/20), 2.53 ± 0.586 (7D: 60% glass, 2.5% FS 40/40/20), and 2.17 ± 0.166 (8D: 60% glass, 3.0% FS 40/40/20).

3.3 Low viscosity monomers

3.3.1 Varied low stress Monomers

Figures 12-17 compare the effect of adding different low viscosity monomers in constant amounts to the continuous phase. Figures 12-14 compare the effects of HEMA and HPMA on flexural strength and fracture toughness for the different low stress monomers. Figures 15-17 show the effect on flexural strength and fracture toughness by adding 1 w/w% 10-MDP to the total mass of formulations with different low stress monomers.

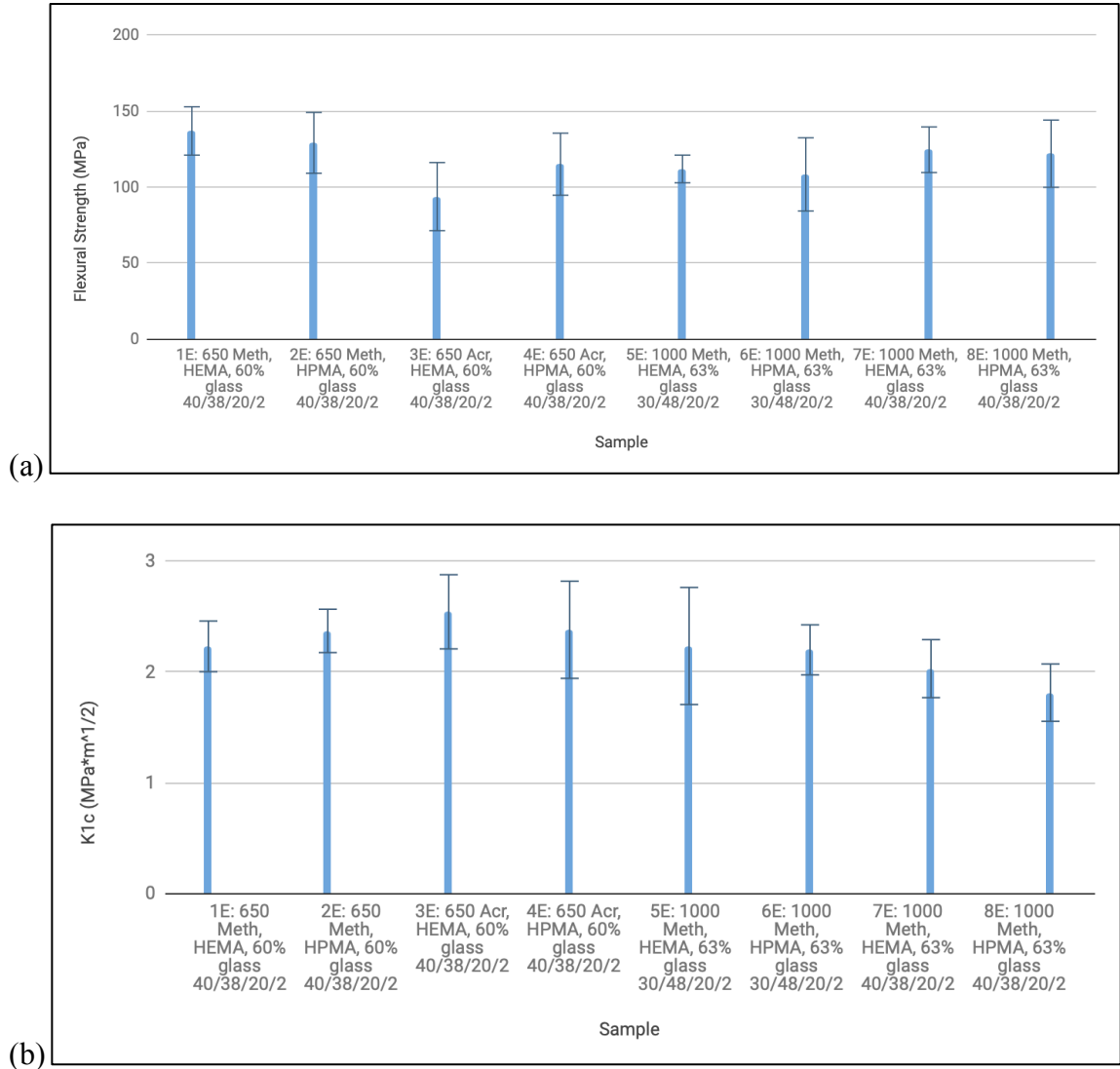


Figure 12. In Figure (a) the flexural strength; and Figure (b) the fracture toughness of formulations where the chemical identity of three different low stress monomers changed in the continuous phase of each formulation. Each of the formulations contained 2 w/w% of a low viscosity monomer, HEMA or HPMA, within the continuous phase. Each formulation was loaded with 60 or 63 w/w% glass, 2.5 w/w% fumed silica, 5 w/w% microcapsules, and a continuous phase ratio of UDMA/TEGMA/LSM/LVM of either 40/38/20/2 or 30/48/20/2.

In Figure 12 (a) the flexural strength; and Figure 12 (b) the fracture toughness of formulations where the chemical identity of three different low stress monomers changed in the continuous phase of each formulation. Each of the formulations contained 2 w/w% of a low viscosity monomer, HEMA or HPMA, within the continuous phase. Each formulation was loaded with 60 or 63 w/w% glass, 2.5 w/w% fumed silica, 5 w/w% microcapsules, and a continuous phase ratio of UDMA/TEGMA/LSM/LVM of either 40/38/20/2 or 30/48/20/2. For flexural strength, the following averages and standard deviations (in MPa) were determined for the various formulations: 136.91±15.9 (1E: 650 Meth, HEMA, 60% glass 40/38/20/2), 129.08±20.0 (2E: 650 Meth, HPMA, 60% glass 40/38/20/2), 93.72±22.4 (3E: 650 Acr, HEMA, 60% glass 40/38/20/2), 115.04±20.4 (4E: 650 Acr, HPMA, 60% glass 40/38/20/2), 111.91±9.1 (5E: 1000 Meth, HEMA, 63% glass 30/48/20/2), 108.33±24.1 (6E: 1000 Meth, HPMA, 63% glass 30/48/20/2), 124.55±15.0 (7E: 1000 Meth, HEMA, 63% glass 40/38/20/2), and 121.96±22.1 (8E: 1000 Meth, HPMA, 63% glass 40/38/20/2). For fracture toughness, the following K_{IC} averages and standard deviations (in MPa*m^{1/2}) were determined for the various formulations: 2.23±0.229 (1E: 650 Meth, HEMA, 60% glass 40/38/20/2), 2.37±0.2 (2E: 650 Meth, HPMA, 60% glass 40/38/20/2), 2.54±0.335 (3E: 650 Acr, HEMA, 60% glass 40/38/20/2), 2.38±0.439 (4E: 650 Acr, HPMA, 60% glass 40/38/20/2), 2.24±0.53 (5E: 1000 Meth, HEMA, 63% glass 30/48/20/2), 2.2±0.226 (6E: 1000 Meth, HPMA, 63% glass 30/48/20/2), 2.03±0.263 (7E: 1000 Meth, HEMA, 63% glass 40/38/20/2), and 1.81±0.259 (8E: 1000 Meth, HPMA, 63% glass 40/38/20/2).

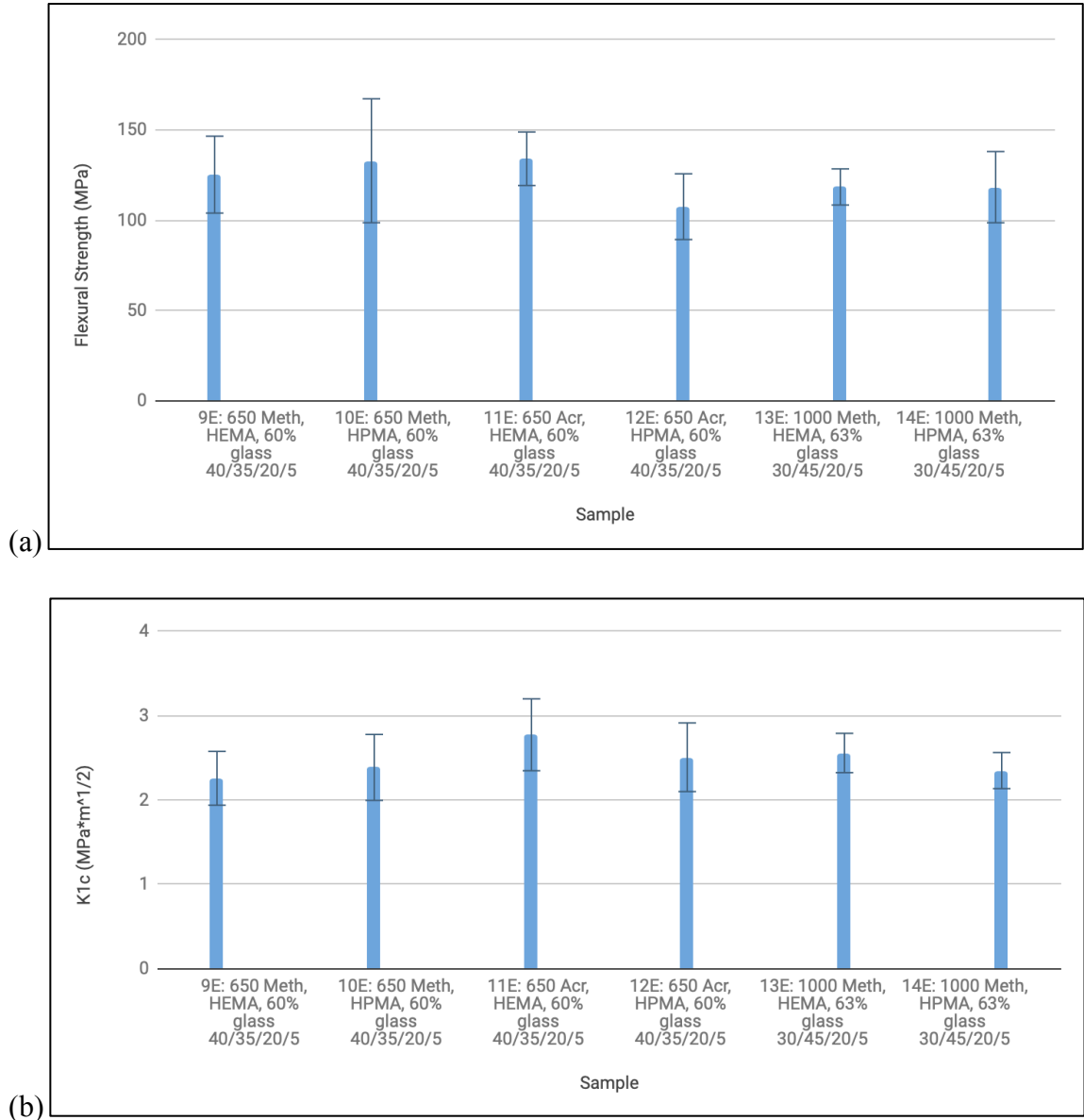


Figure 13. In Figure (a) the flexural strength; and Figure (b) the fracture toughness of formulations where the chemical identity of three different low stress monomers changed in the continuous phase of each formulation. Each of the formulations contained 5 w/w% of a low viscosity monomer, HEMA or HPMA, within the continuous phase. Each formulation was loaded with 60 or 63 w/w% glass, 2.5 w/w% fumed silica, 5 w/w% microcapsules, and a continuous phase ratio of UDMA/TEGMA/LSM/LVM of either 40/35/20/5 or 30/45/20/5.

Figure 13 (a) and (b) differ from Figure 12 (a) and (b) in that HEMA or HPMA was increased from 2 to 5 w/w%. For flexural strength, the following averages and standard deviations (in MPa) were determined for the various formulations: 125.15±21.3 (9E: 650 Meth, HEMA, 60% glass 40/35/20/5), 132.83±34.3 (10E: 650 Meth, HPMA, 60% glass 40/35/20/5), 133.94±14.8 (11E: 650 Acr, HEMA, 60% glass 40/35/20/5), 107.41±18.2 (12E: 650 Acr, HPMA, 60% glass 40/35/20/5), 118.34±10.0 (13E: 1000 Meth, HEMA, 63% glass 30/45/20/5), and 118.22±19.7 (14E: 1000 Meth, HPMA, 63% glass 30/45/20/5). For fracture toughness, the following K_{IC} averages and standard deviations (in MPa*m^{1/2}) were determined for the various formulations: 2.26±0.319 (9E: 650 Meth, HEMA, 60% glass 40/35/20/5), 2.38±0.391 (10E: 650 Meth, HPMA, 60% glass 40/35/20/5), 2.77±0.426 (11E: 650 Acr, HEMA, 60% glass 40/35/20/5), 2.51±0.407 (12E: 650 Acr, HPMA, 60% glass 40/35/20/5), 2.56±0.233 (13E: 1000 Meth, HEMA, 63% glass 30/45/20/5), and 2.35±0.214 (14E: 1000 Meth, HPMA, 63% glass 30/45/20/5).

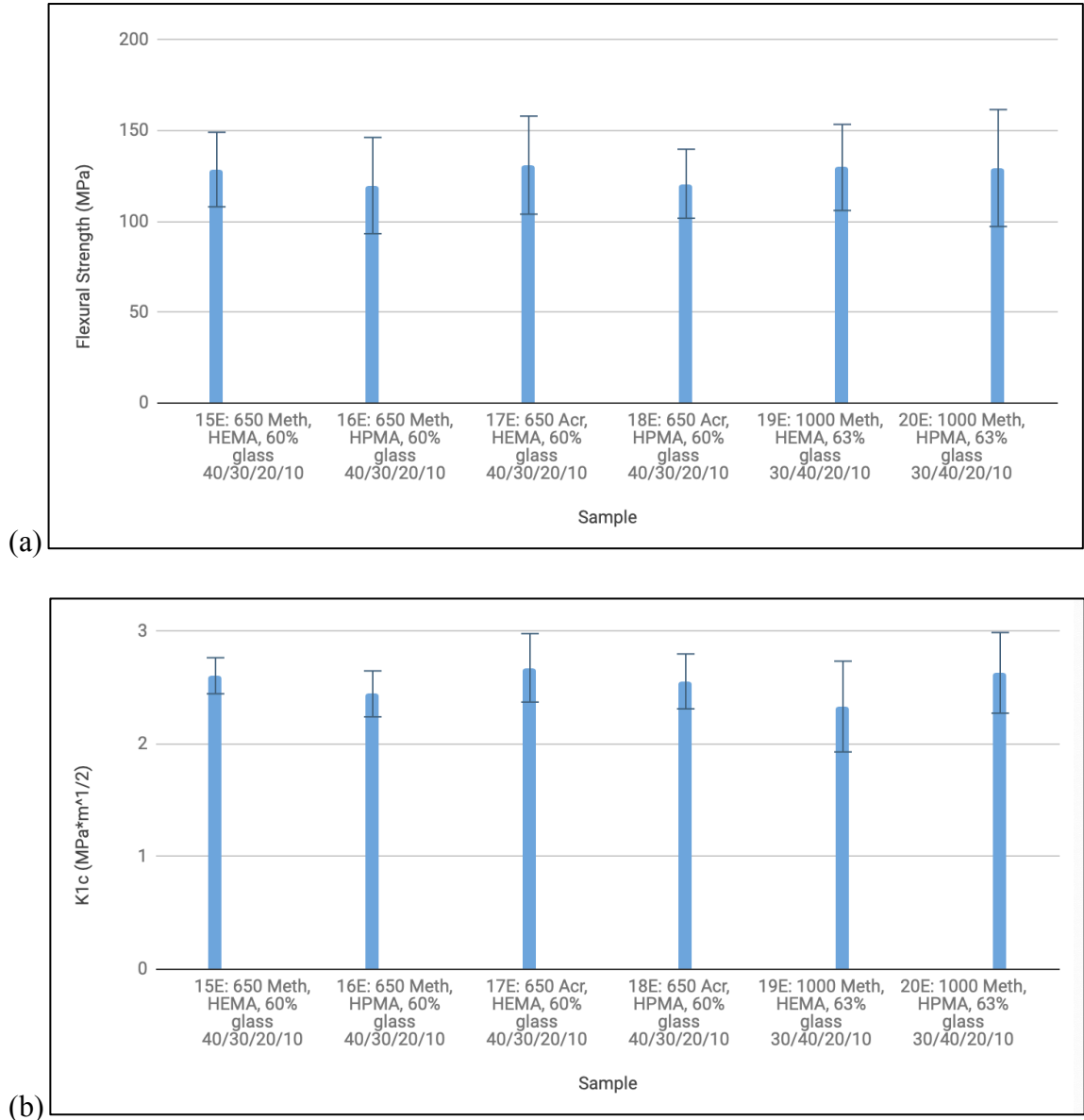


Figure 14. In Figure (a) the flexural strength; and Figure (b) the fracture toughness of formulations where the chemical identity of three different low stress monomers changed in the continuous phase of each formulation. Each of the formulations contained 10 w/w% of a low viscosity monomer, HEMA or HPMA, within the continuous phase. Each formulation was loaded with 60 or 63 w/w% glass, 2.5 w/w% fumed silica, 5 w/w% microcapsules, and a continuous phase ratio of UDMA/TEGMA/LSM/LVM of either 40/30/20/10 or 30/40/20/10.

Figure 14 (a) and (b) differ from Figure 12 (a) and (b) in that HEMA or HPMA was increased from 2 to 10 w/w%. For flexural strength, the following averages and standard deviations (in MPa) were determined for the various formulations: 128.46±20.5 (15E: 650 Meth, HEMA, 60% glass 40/30/20/10), 119.63±26.5 (16E: 650 Meth, HPMA, 60% glass 40/30/20/10), 130.88±27.0 (17E: 650 Acr, HEMA, 60% glass 40/30/20/10), 120.64±19.0 (18E: 650 Acr, HPMA, 60% glass 40/30/20/10), 129.62±23.7 (19E: 1000 Meth, HEMA, 63% glass 30/40/20/10), and 129.29±32.2 (20E: 1000 Meth, HPMA, 63% glass 30/40/20/10). For fracture toughness, the following K_{IC} averages and standard deviations (in MPa*m^{1/2}) were determined for the various formulations: 2.6±0.16 (15E: 650 Meth, HEMA, 60% glass 40/30/20/10), 2.44±0.204 (16E: 650 Meth, HPMA, 60% glass 40/30/20/10), 2.67±0.304 (17E: 650 Acr, HEMA, 60% glass 40/30/20/10), 2.55±0.244 (18E: 650 Acr, HPMA, 60% glass 40/30/20/10), 2.33±0.404 (19E: 1000 Meth, HEMA, 63% glass 30/40/20/10), and 2.63±0.358 (20E: 1000 Meth, HPMA, 63% glass 30/40/20/10).

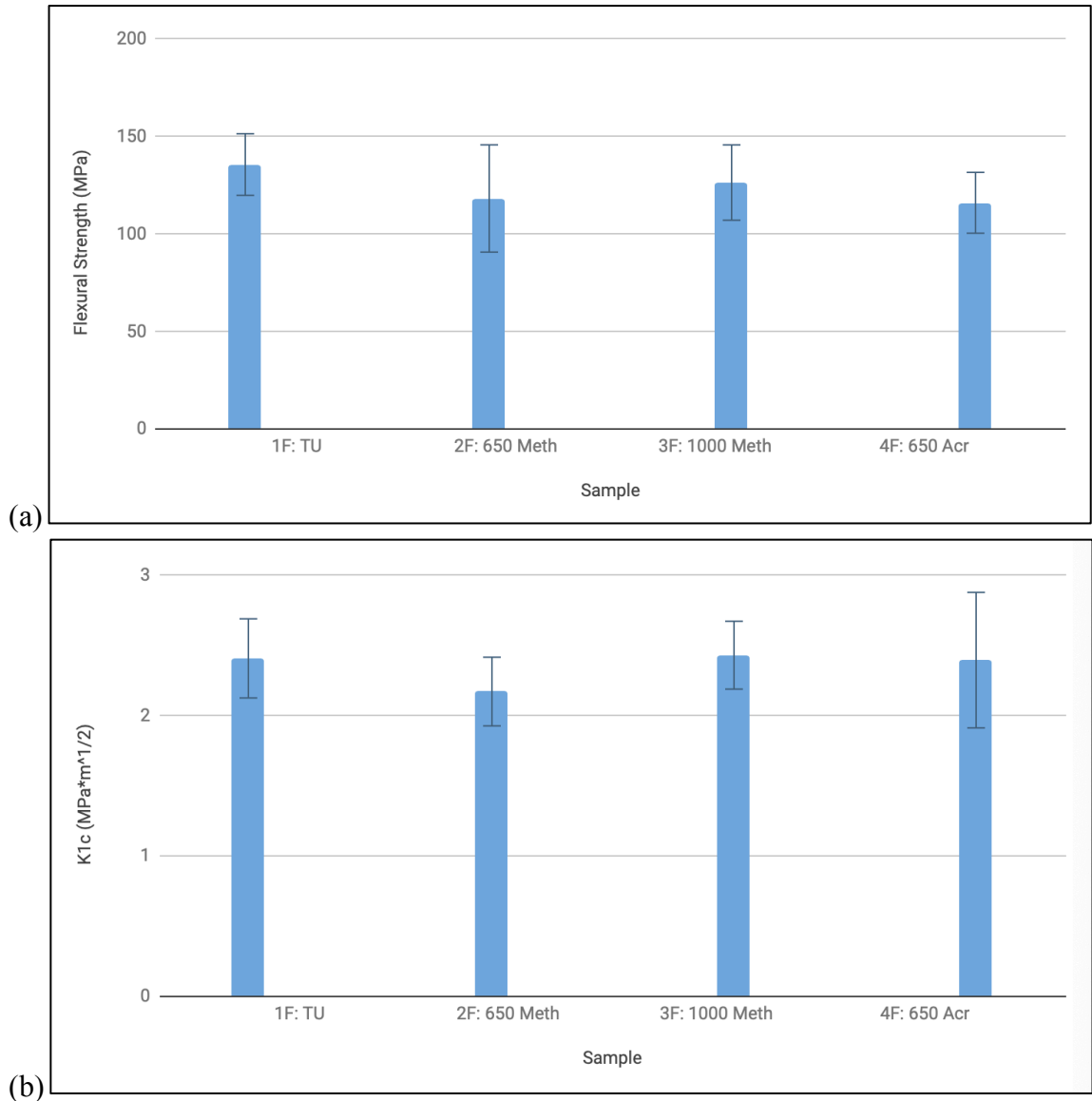


Figure 15. In Figure (a) the flexural strength; and Figure (b) the fracture toughness of formulations where the chemical identity of four different low stress monomers changed in the continuous phase of each formulation. Each formulation was loaded with 60 w/w% glass, 2.0 w/w% fumed silica, 5 w/w% microcapsules, addition of 1w/w% 10-MDP of the total formulation mass and a continuous phase ratio of UDMA/TEGMA/LSM of 40/40/20.

In Figure 15 (a) the flexural strength; and Figure 15 (b) the fracture toughness of formulations where the chemical identity of four different low stress monomers changed in the continuous phase of each formulation. Each formulation was loaded with 60 w/w% glass, 2.0 w/w% fumed silica, 5 w/w% microcapsules, addition of 1w/w% 10-MDP of the total formulation mass and a continuous phase ratio of UDMA/TEGMA/LSM of 40/40/20. For flexural strength, the following averages and standard deviations (in MPa) were determined for the various formulations: 135.47 ± 15.8 (1F: TU), 118.07 ± 27.5 (2F: 650 Meth), 126.24 ± 19.3 (3F: 1000 Meth), and 115.86 ± 15.6 (4F: 650 Acr). For fracture toughness, the following K_{IC} averages and standard deviations (in $\text{MPa} \cdot \text{m}^{1/2}$) were determined for the various formulations: 2.41 ± 0.282 (1F: TU), 2.17 ± 0.245 (2F: 650 Meth), 2.43 ± 0.242 (3F: 1000 Meth), and 2.39 ± 0.483 (4F: 650 Acr).

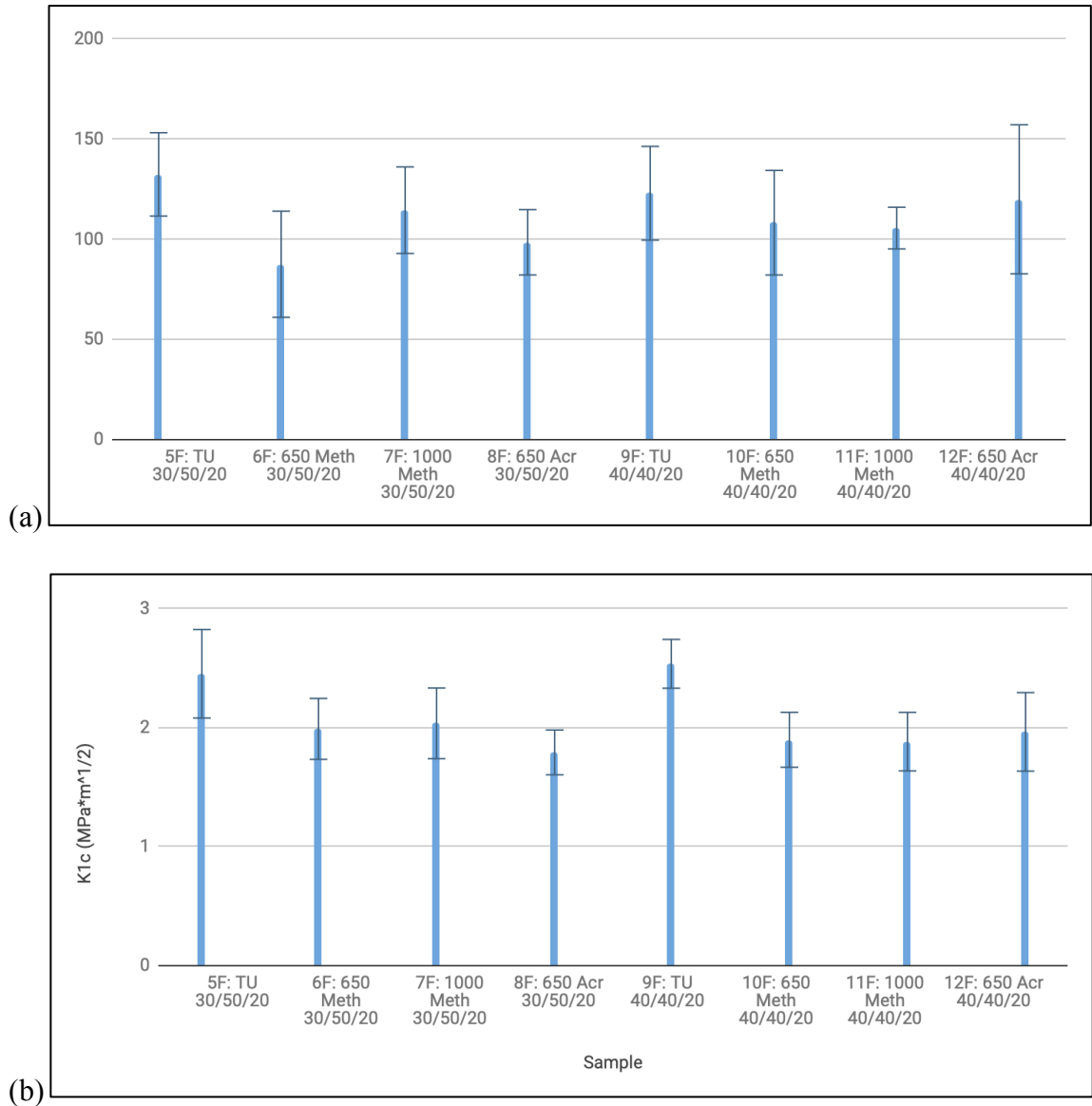


Figure 16. In Figure (a) the flexural strength; and figure (b) the fracture toughness of formulations where the chemical identity of four different low stress monomers changed in the continuous phase of each formulation. Each formulation was loaded with 60 w/w% glass, 2.5 w/w% fumed silica, 5 w/w% microcapsules, addition of 1w/w% 10-MDP of the total formulation mass and a continuous phase ratio of UDMA/TEGMA/LSM of either 40/40/20 or 30/50/20.

Figure 16 (a) and (b) differs from Figure 15 (a) and (b) in that fumed silica was increased from 2.0 w/w% FS to 2.5w/w% FS and the continuous phase ratio 30/50/20 was also included. For flexural strength, the following averages and standard deviations (in MPa) were determined for the various formulations: 132.28 ± 20.8 (5F: TU 30/50/20), 87.4 ± 26.5 (6F: 650 Meth 30/50/20), 114.39 ± 21.6 (7F: 1000 Meth 30/50/20), 98.37 ± 16.3 (8F: 650 Acr 30/50/20), 122.84 ± 23.4 (9F: TU 40/40/20), 108.16 ± 26.1 (10F: 650 Meth 40/40/20), 105.47 ± 10.4 (11F: 1000 Meth 40/40/20), and 119.82 ± 37.2 (12F: 650 Acr 40/40/20). For fracture toughness, the following K_{IC} averages and standard deviations (in $\text{MPa} \cdot \text{m}^{1/2}$) were determined for the various formulations: 2.45 ± 0.372 (5F: TU 30/50/20), 1.99 ± 0.256 (6F: 650 Meth 30/50/20), 2.03 ± 0.297 (7F: 1000 Meth 30/50/20), 1.79 ± 0.188 (8F: 650 Acr 30/50/20), 2.54 ± 0.205 (9F: TU 40/40/20), 1.9 ± 0.231 (10F: 650 Meth 40/40/20), 1.88 ± 0.246 (11F: 1000 Meth 40/40/20), and 1.96 ± 0.33 (12F: 650 Acr 40/40/20).

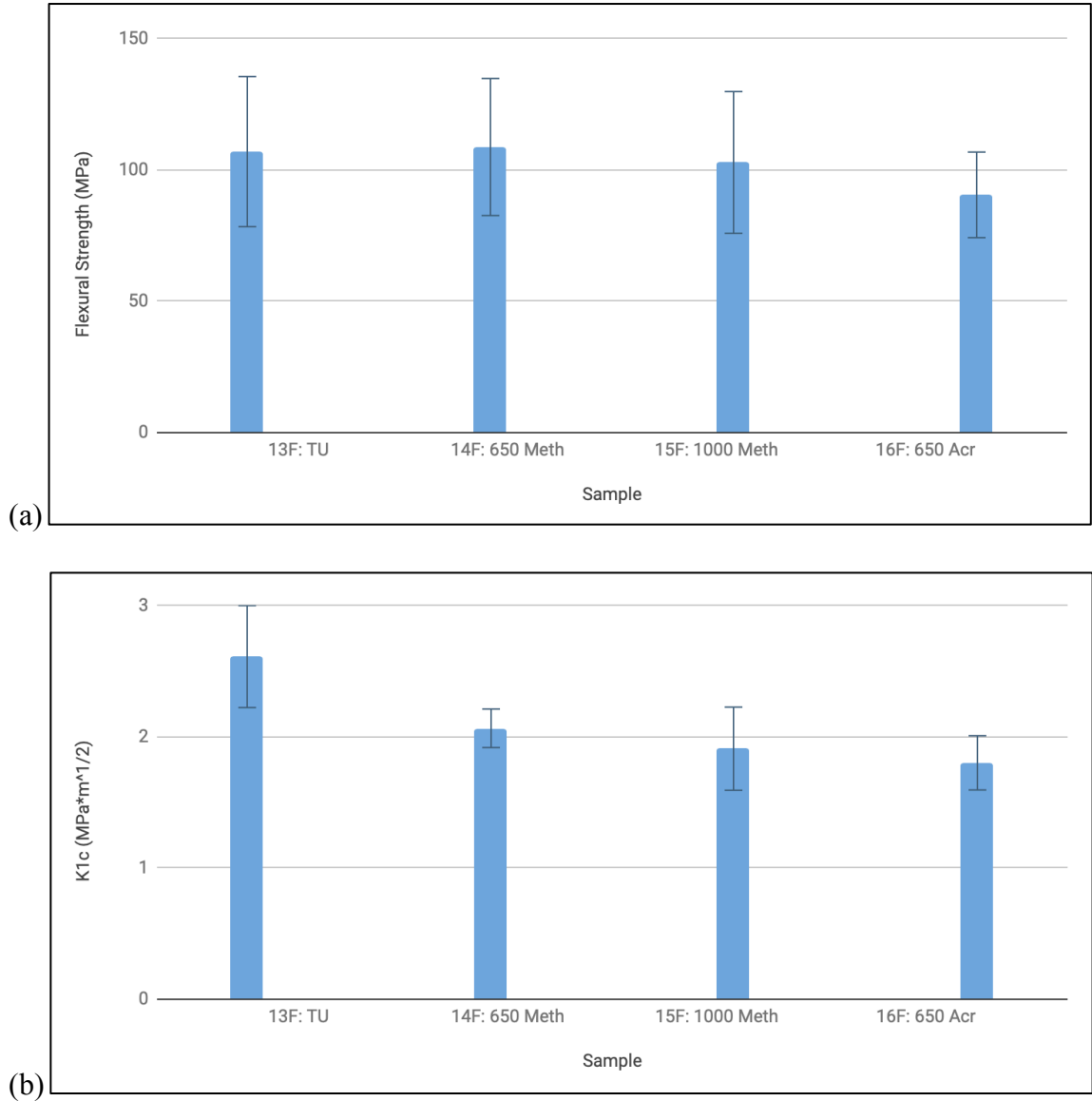


Figure 17. In Figure (a) the flexural strength; and Figure (b) the fracture toughness of formulations where the chemical identity of four different low stress monomers changed in the continuous phase of each formulation. Each formulation was loaded with 60 w/w% glass, 3.0 w/w% fumed silica, 5 w/w% microcapsules, addition of 1w/w% 10-MDP of the total formulation mass and a continuous phase ratio of UDMA/TEGMA/LSM of 40/40/20.

Figure 17 (a) and (b) differ from Figure 15 (a) and (b) in that the fumed silica is increased from 2.0 w/w% to 3.0 w/w%. For flexural strength, the following averages and standard deviations (in MPa) were determined for the various formulations: 106.9 ± 28.6 (13F: TU), 108.66 ± 26.1 (14F: 650 Meth), 102.78 ± 27.0 (15F: 1000 Meth), and 90.44 ± 16.3 (16F: 650 Acr). For fracture toughness, the following K_{IC} averages and standard deviations (in $\text{MPa} \cdot \text{m}^{1/2}$) were determined for the various formulations: 2.61 ± 0.389 (13F: TU), 2.06 ± 0.147 (14F: 650 Meth), 1.91 ± 0.317 (15F: 1000 Meth), and 1.8 ± 0.207 (16F: 650 Acr).

3.3.2 Low viscosity monomers

Figures 18-20 show the effect of 2, 5, and 10 w/w% HEMA or HPMA on flexural strength and fracture toughness. In the following graphs the type and amount of low stress monomer within the continuous phase is constant while the type and amount of low viscosity monomer within the continuous phase was changed.

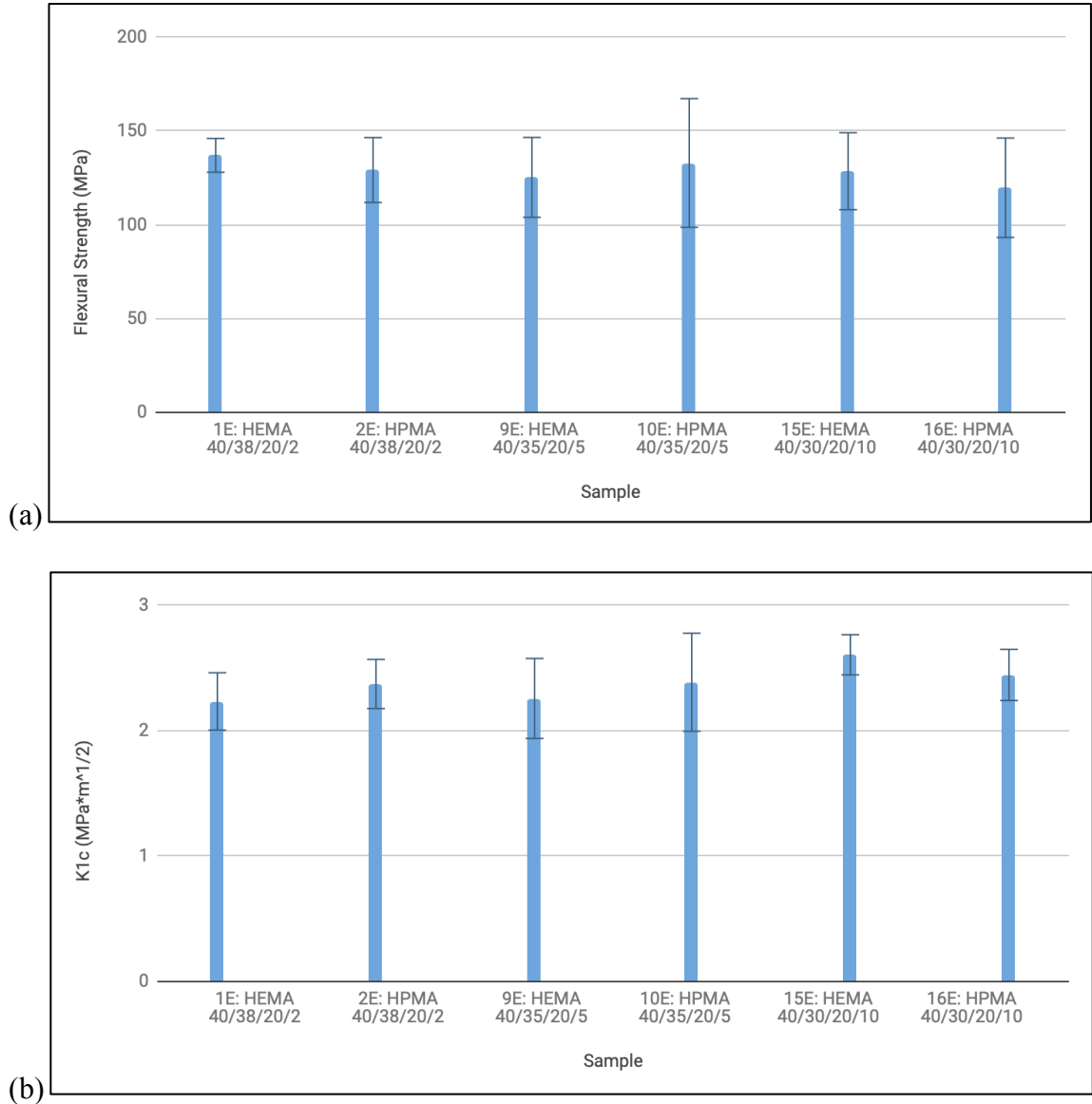


Figure 18. In Figure (a) the flexural strength; and Figure (b) the fracture toughness of formulations where the amount of Terathane 650 extended urethane methacrylate was held constant while amount of the low viscosity monomer differed as either 2,5, or 10 w/w% of HEMA or HPMA in the continuous phase of each formulation. Each formulation was loaded with 60 w/w% glass, 2.5 w/w% fumed silica, 5 w/w% microcapsules, and a continuous phase ratio of UDMA/TEGMA/LSM/LVM of either 40/38/20/2, 40/35/20/5, or 40/30/20/10.

In Figure 18 (a) the flexural strength; and Figure 18 (b) the fracture toughness of formulations where the amount of Terathane 650 extended urethane methacrylate was held constant while amount of the low viscosity monomer differed as either 2,5, or 10 w/w% of HEMA or HPMA in the continuous phase of each formulation. Each formulation was loaded with 60 w/w% glass, 2.5 w/w% fumed silica, 5 w/w% microcapsules, and a continuous phase ratio of UDMA/TEGMA/LSM/LVM of either 40/38/20/2, 40/35/20/5, or 40/30/20/10. For flexural strength, the following averages and standard deviations (in MPa) were determined for the various formulations: 136.91 ± 9.0 (1E: HEMA 40/38/20/2), 129.08 ± 17.3 (2E: HPMA 40/38/20/2), 125.15 ± 21.3 (9E: HEMA 40/35/20/5), 132.83 ± 34.3 (10E: HPMA 40/35/20/5), 128.46 ± 20.5 (15E: HEMA 40/30/20/10), and 119.63 ± 26.5 (16E: HPMA 40/30/20/10). For fracture toughness, the following K_{IC} averages and standard deviations (in $\text{MPa} \cdot \text{m}^{1/2}$) were determined for the various formulations: 2.23 ± 0.229 (1E: HEMA 40/38/20/2), 2.37 ± 0.2 (2E: HPMA 40/38/20/2), 2.26 ± 0.319 (9E: HEMA 40/35/20/5), 2.38 ± 0.391 (10E: HPMA 40/35/20/5), 2.6 ± 0.16 (15E: HEMA 40/30/20/10), and 2.44 ± 0.204 (16E: HPMA 40/30/20/10).

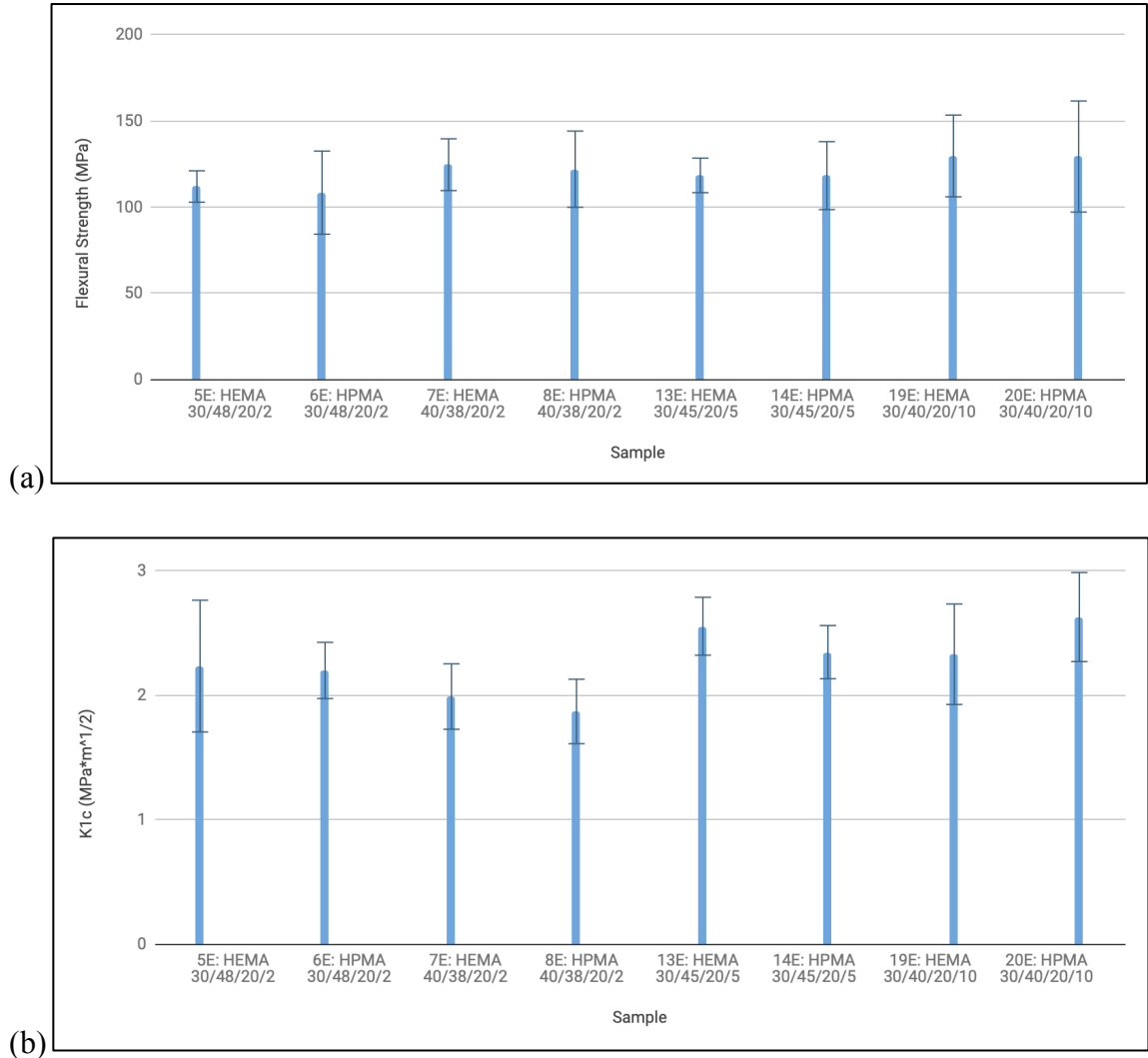


Figure 19. In Figure (a) the flexural strength; and Figure (b) the fracture toughness of formulations where the amount of Terathane 1000 extended urethane methacrylate was held constant while amount of the low viscosity monomer differed as either 2, 5, or 10 w/w% of HEMA or HPMA in the continuous phase of each formulation. Each formulation was loaded with 63 w/w% glass, 2.5 w/w% fumed silica, 5 w/w% microcapsules, and a continuous phase ratio of UDMA/TEGMA/LSM/LVM of either 30/48/20/2, 40/38/20/2, 30/45/20/5, or 30/40/20/10.

Figure 19 (a) and (b) differs from Figure 18 (a) and (b) by changing 650 Meth with 1000 Meth. For flexural strength, the following averages and standard deviations (in MPa) were determined for the various formulations: 111.91±24.1 (5E: HEMA 30/48/20/2), 108.33±9.1 (6E: HPMA 30/48/20/2), 124.55±22.1 (7E: HEMA 40/38/20/2), 121.96±15.0 (8E: HPMA 40/38/20/2), 118.34±10.0 (13E: HEMA 30/45/20/5), 118.22±19.7 (14E: HPMA 30/45/20/5), 129.62±23.7 (19E: HEMA 30/40/20/10), and 129.29±32.2 (20E: HPMA 30/40/20/10). For fracture toughness, the following K_{IC} averages and standard deviations (in MPa*m^{1/2}) were determined for the various formulations: 2.24±0.53 (5E: HEMA 30/48/20/2), 2.2±0.226 (6E: HPMA 30/48/20/2), 1.99±0.263 (7E: HEMA 40/38/20/2), 1.87±0.259 (8E: HPMA 40/38/20/2), 2.56±0.233 (13E: HEMA 30/45/20/5), 2.35±0.214 (14E: HPMA 30/45/20/5), 2.33±0.404 (19E: HEMA 30/40/20/10), and 2.63±0.358 (20E: HPMA 30/40/20/10).

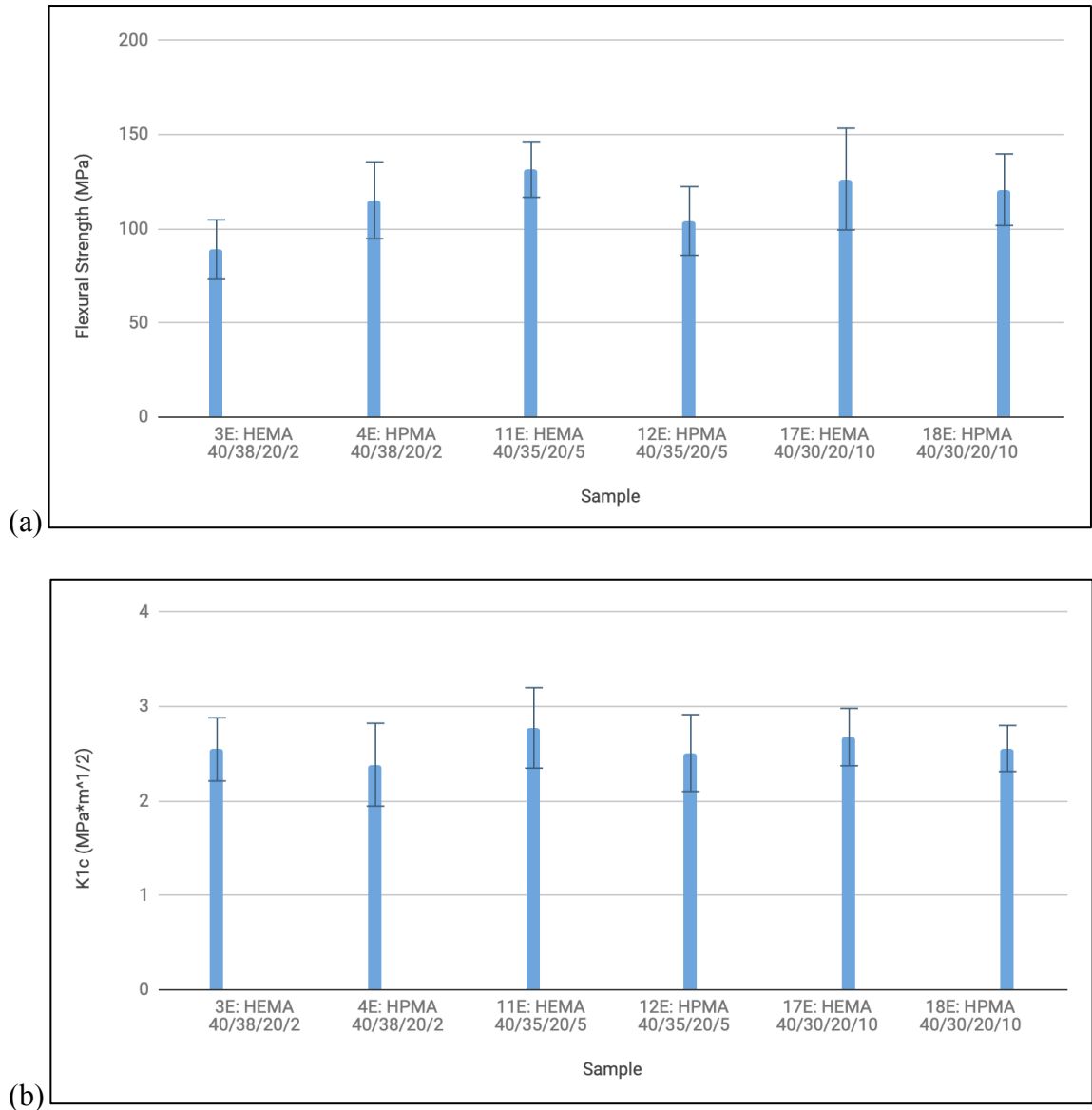


Figure 20. In Figure (a) the flexural strength; and Figure (b) the fracture toughness of formulations where the amount of Terathane 650 extended urethane acrylate was held constant while amount of the low viscosity monomer differed as either 2,5, or 10 w/w% of HEMA or HPMA in the continuous phase of each formulation. Each formulation was loaded with 60 w/w% glass, 2.5 w/w% fumed silica, 5 w/w% microcapsules, and a continuous phase ratio of UDMA/TEGMA/LSM/LVM of either 40/38/20/2, 40/35/20/5, or 40/30/20/10.

Figure 20 (a) and (b) differs from Figure 18 (a) and (b) by changing 650 Meth with 650 Acr. For flexural strength, the following averages and standard deviations (in MPa) were determined for the various formulations: 88.81 ± 20.4 (3E: HEMA 40/38/20/2), 115.04 ± 15.8 (4E: HPMA 40/38/20/2), 131.44 ± 14.8 (11E: HEMA 40/35/20/5), 104.06 ± 18.2 (12E: HPMA 40/35/20/5), 126.29 ± 27.0 (17E: HEMA 40/30/20/10), and 120.64 ± 19.0 (18E: HPMA 40/30/20/10). For fracture toughness, the following K_{IC} averages and standard deviations (in $\text{MPa} \cdot \text{m}^{1/2}$) were determined for the various formulations: 2.54 ± 0.335 (3E: HEMA 40/38/20/2), 2.38 ± 0.439 (4E: HPMA 40/38/20/2), 2.77 ± 0.426 (11E: HEMA 40/35/20/5), 2.51 ± 0.407 (12E: HPMA 40/35/20/5), 2.67 ± 0.304 (17E: HEMA 40/30/20/10), and 2.55 ± 0.244 (18E: HPMA 40/30/20/10).

3.3.3 Fumed silica

Figures 21-24 compare the effect of fumed silica on flexural strength and fracture toughness for the different low stress monomers.

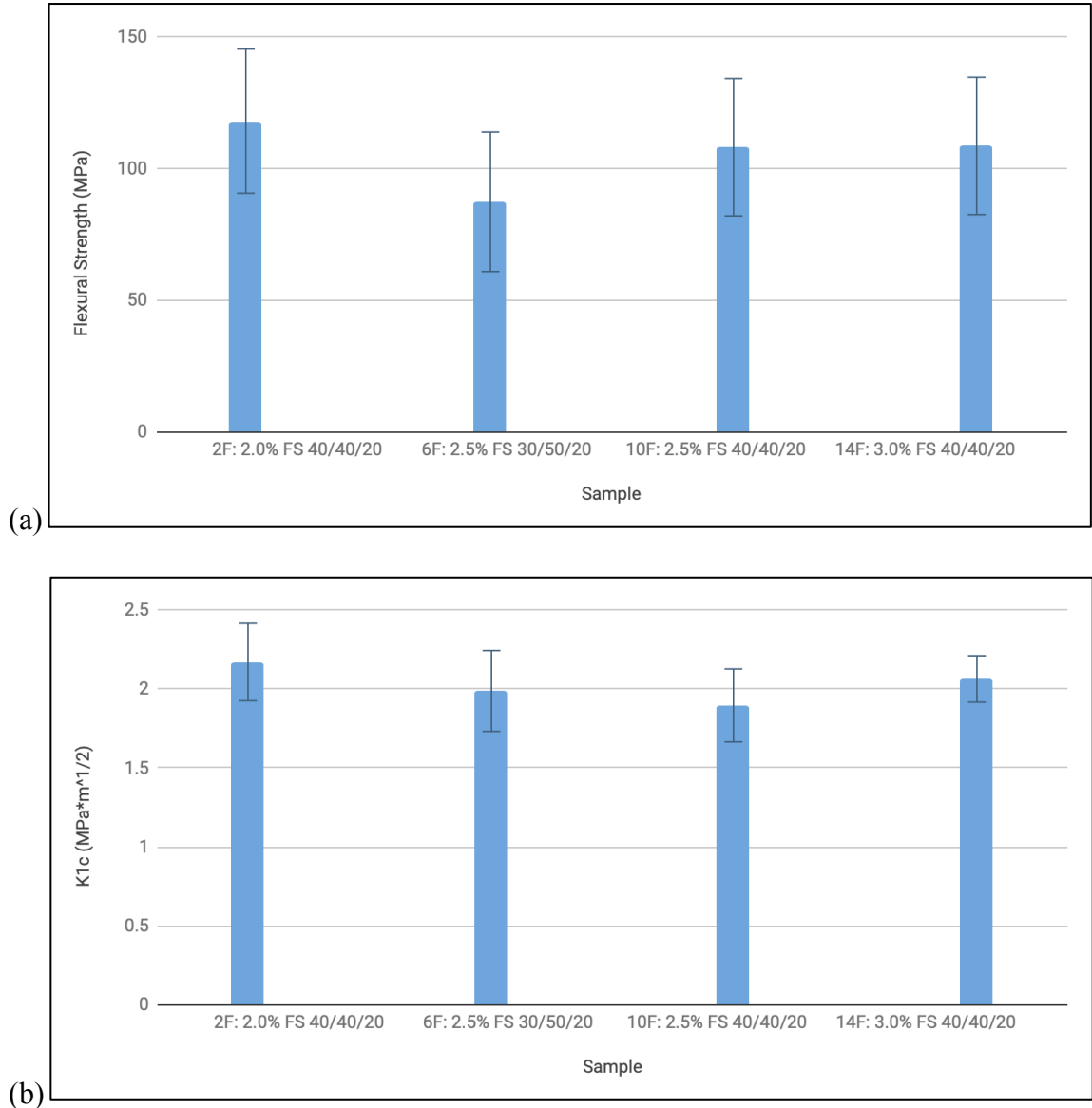


Figure 21. In Figure (a) the flexural strength; and Figure (b) the fracture toughness of formulations where each was created using Terathane 650 extended urethane methacrylate as the low stress monomer. Each formulation was loaded with 60 w/w% glass, 2.0, 2.5, or 3.0 w/w% fumed silica, 5 w/w% microcapsules, 1 w/w% 10-MDP of the total formulation mass, and a continuous phase ratio of UDMA/TEGMA/LSM of either 30/50/20 or 40/40/20.

In Figure 21 (a) the flexural strength; and Figure 21 (b) the fracture toughness of formulations where each was created using Terathane 650 extended urethane methacrylate as the low stress monomer. Each formulation was loaded with 60 w/w% glass, 2.0, 2.5, or 3.0 w/w% fumed silica, 5 w/w% microcapsules, 1 w/w% 10-MDP of the total formulation mass, and a continuous phase ratio of UDMA/TEGMA/LSM of either 30/50/20 or 40/40/20. For flexural strength, the following averages and standard deviations (in MPa) were determined for the various formulations: 118.07 ± 27.5 (2F: 2.0% FS 40/40/20), 87.4 ± 26.5 (6F: 2.5% FS 30/50/20), 108.16 ± 26.1 (10F: 2.5% FS 40/40/20), and 108.66 ± 26.1 (14F: 3.0% FS 40/40/20). For fracture toughness, the following K_{IC} averages and standard deviations (in $\text{MPa} \cdot \text{m}^{1/2}$) were determined for the various formulations: 2.17 ± 0.245 (2F: 2.0% FS 40/40/20), 1.99 ± 0.256 (6F: 2.5% FS 30/50/20), 1.9 ± 0.231 (10F: 2.5% FS 40/40/20), and 2.06 ± 0.147 (14F: 3.0% FS 40/40/20).

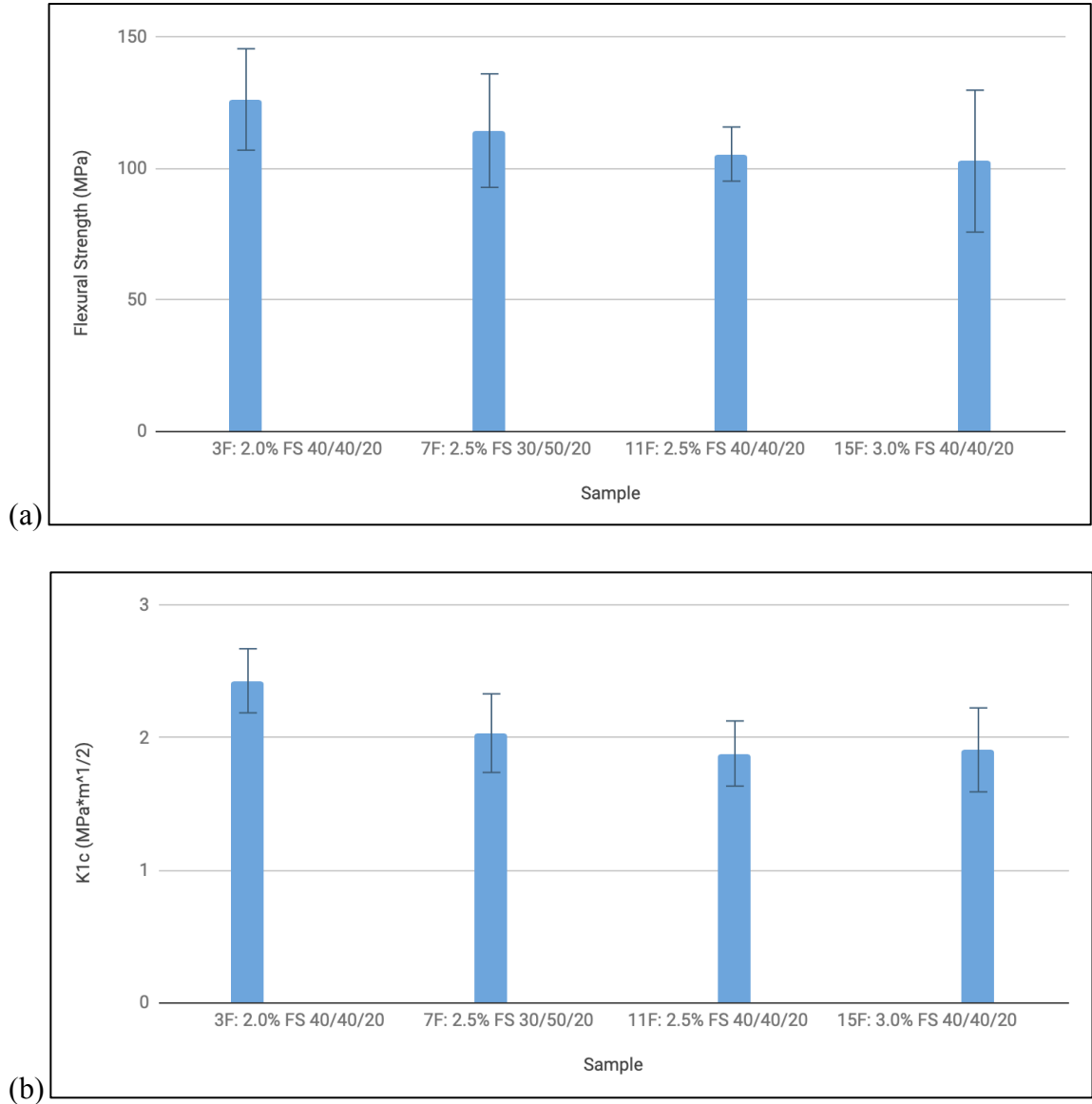


Figure 22. In Figure (a) the flexural strength; and Figure (b) the fracture toughness of formulations where each was created using Terathane 1000 extended urethane methacrylate as the low stress monomer. Each formulation was loaded with 60 w/w% glass, 2.0, 2.5, or 3.0 w/w% fumed silica, 5 w/w% microcapsules, 1 w/w% 10-MDP of the total formulation mass, and a continuous phase ratio of UDMA/TEGMA/LSM of either 30/50/20 or 40/40/20.

Figure 22 (a) and (b) differ from Figure 21 (a) and (b) by changing 650 Meth with 1000 Meth. For flexural strength, the following averages and standard deviations (in MPa) were determined for the various formulations: 126.24 ± 19.3 (3F: 2.0% FS 40/40/20), 114.39 ± 21.6 (7F: 2.5% FS 30/50/20), 105.47 ± 10.4 (11F: 2.5% FS 40/40/20), and 102.78 ± 27.0 (15F: 3.0% FS 40/40/20). For fracture toughness, the following K_{IC} averages and standard deviations (in $\text{MPa} \cdot \text{m}^{1/2}$) were determined for the various formulations: 2.43 ± 0.242 (3F: 2.0% FS 40/40/20), 2.03 ± 0.297 (7F: 2.5% FS 30/50/20), 1.88 ± 0.246 (11F: 2.5% FS 40/40/20), and 1.91 ± 0.317 (15F: 3.0% FS 40/40/20).

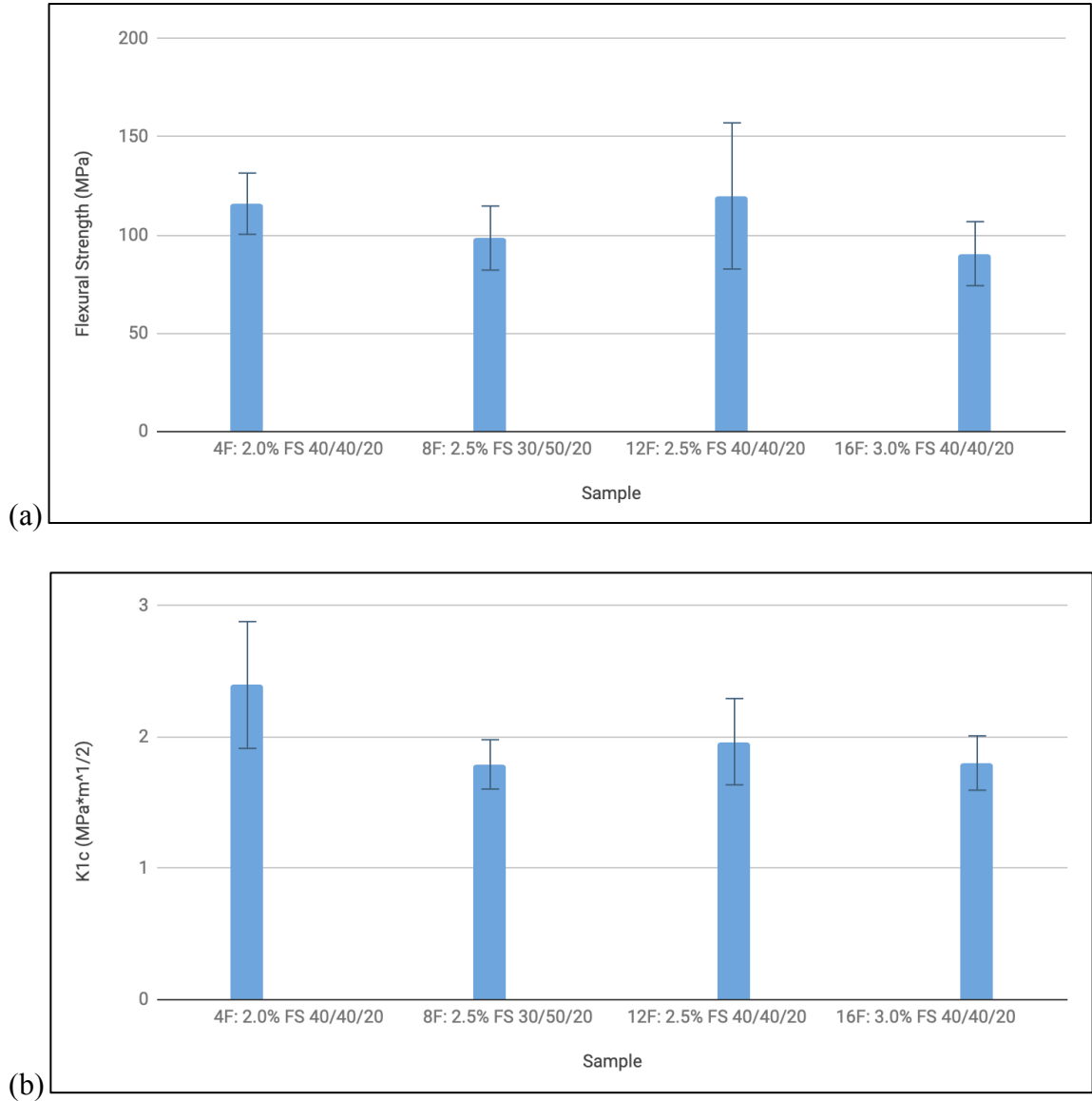


Figure 23. In Figure (a) the flexural strength; and Figure (b) the fracture toughness of formulations where each was created using Terathane 650 extended urethane acrylate as the low stress monomer. Each formulation was loaded with 60 w/w% glass, 2.0, 2.5, or 3.0 w/w% fumed silica, 5 w/w% microcapsules, 1 w/w% 10-MDP of the total formulation mass, and a continuous phase ratio of UDMA/TEGMA/LSM of either 30/50/20 or 40/40/20.

Figure 23 (a) and (b) differ from Figure 21 (a) and (b) by changing 650 Meth with 650 Acr. For flexural strength, the following averages and standard deviations (in MPa) were determined for the various formulations: 115.86 ± 15.6 (4F: 2.0% FS 40/40/20), 98.37 ± 16.3 (8F: 2.5% FS 30/50/20), 119.82 ± 37.2 (12F: 2.5% FS 40/40/20), and 90.44 ± 16.3 (16F: 3.0% FS 40/40/20). For fracture toughness, the following K_{IC} averages and standard deviations (in $\text{MPa} \cdot \text{m}^{1/2}$) were determined for the various formulations: 2.39 ± 0.483 (4F: 2.0% FS 40/40/20), 1.79 ± 0.188 (8F: 2.5% FS 30/50/20), 1.96 ± 0.33 (12F: 2.5% FS 40/40/20), and 1.8 ± 0.207 (16F: 3.0% FS 40/40/20).

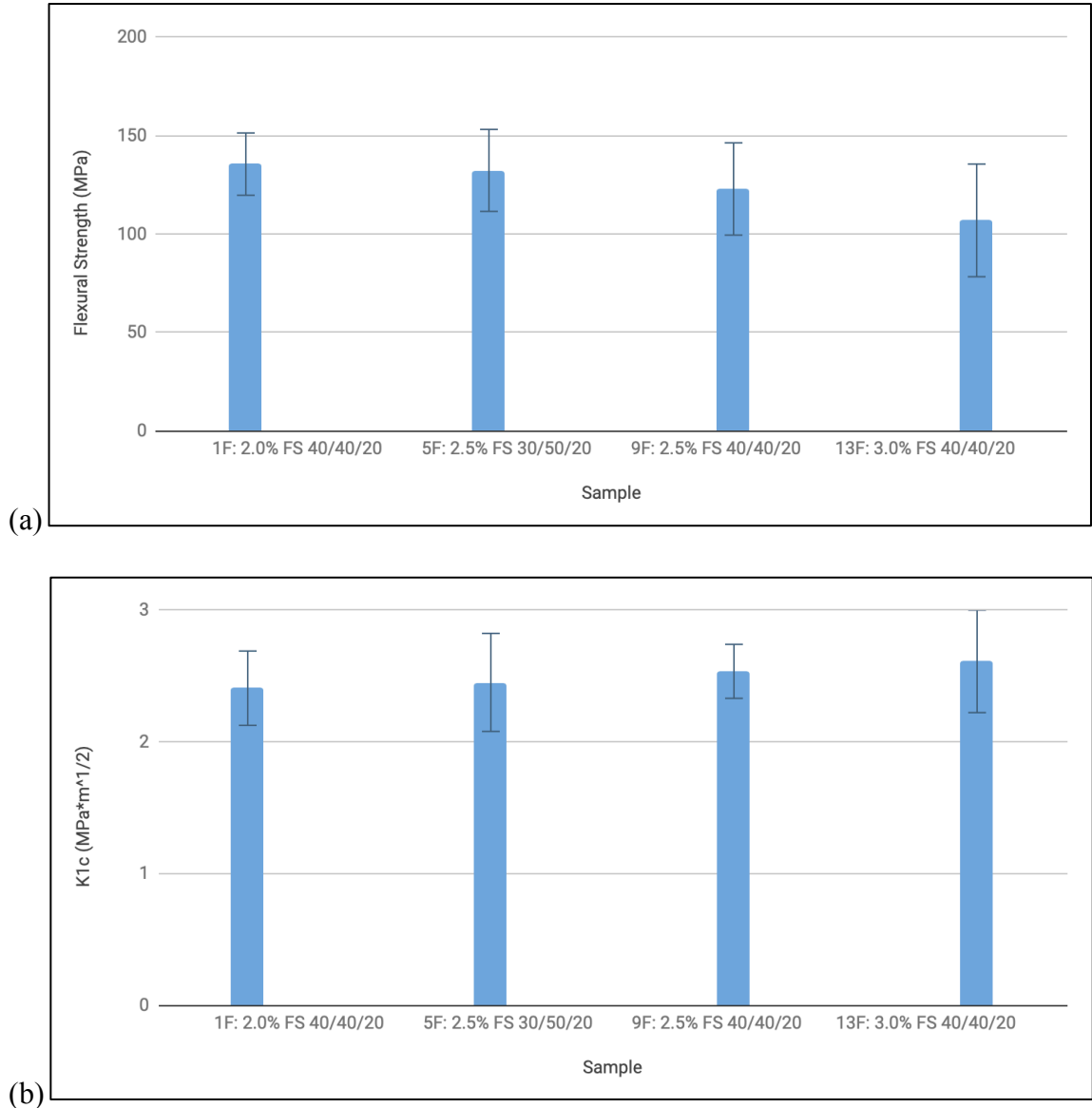


Figure 24: In Figure (a) the flexural strength; and Figure (b) the fracture toughness of formulations where each was created using the thiourethane oligomer as the low stress monomer. Each formulation was loaded with 60 w/w% glass, 2.0, 2.5, or 3.0 w/w% fumed silica, 5 w/w% microcapsules, 1 w/w% 10-MDP of the total formulation mass, and a continuous phase ratio of UDMA/TEGMA/LSM of either 30/50/20 or 40/40/20.

Figure 24 (a) and (b) differ from Figure 21 (a) and (b) by changing 650 Meth with TU. For flexural strength, the following averages and standard deviations (in MPa) were determined for the various formulations: 135.47 ± 15.8 (1F: 2.0% FS 40/40/20), 132.28 ± 20.8 (5F: 2.5% FS 30/50/20), 122.84 ± 23.4 (9F: 2.5% FS 40/40/20), and 106.9 ± 28.6 (13F: 3.0% FS 40/40/20). For fracture toughness, the following K_{IC} averages and standard deviations (in $\text{MPa} \cdot \text{m}^{1/2}$) were determined for the various formulations: 2.41 ± 0.282 (1F: 2.0% FS 40/40/20), 2.45 ± 0.372 (5F: 2.5% FS 30/50/20), 2.54 ± 0.205 (9F: 2.5% FS 40/40/20), and 2.61 ± 0.389 (13F: 3.0% FS 40/40/20).

Chapter 4

Discussion

4.1 Discussion

In this study, the goal was to develop low stress, BPA free, ion eluting formulations with the potential for use as a flowable composite/ base liner. In order to achieve this goal, formulations were developed exploring the effect of different variables on the flexural strength and fracture toughness. The variables include: the type of low stress monomer in the continuous phase, the UDMA/TEGMA ratio within the continuous phase, the amount of glass loaded, the amount of fumed silica loaded, and the inclusion of low viscosity monomers. The effect of combination of these variables were also examined. In dental composites, both filler morphology and filler loading influence the flexural strength and fracture toughness [58]. Flexural strength and fracture toughness are also affected by the composition of the polymer matrix and the coupling between the filler and the matrix [59]. In this study, the trends of variables are examined to see how microcapsules, low stress monomers, and low viscosity monomers in a Bis-GMA free flowable composite compare to those of current dental composites. The hypothesis was that by changing the variables the flexural strength and the fracture toughness of the sample formula would also change by a statistically different amount. The null hypothesis was that there was no statistical difference in flexural strength or fracture toughness between the samples when the variables changed.

4.2 Low stress monomers

4.2.1 Varied low stress monomers

Figures 3-7 demonstrate the effect the different low stress monomers have on the flexural strength and fracture toughness in several different formulations. The hypothesis for these figures was that when the low stress monomer is changed the flexural strength or

fracture toughness also changed. The null hypothesis is that the change in low stress monomer will have no effect on the flexural strength or fracture toughness.

In Figure 3 (a) the sample 3D: TU 40/40/20 was found to be a statistically lower flexural strength than all other samples in that figure except 1B: 1000 Meth 30/50/20. This shows that the lowest flexural strength occurs with TU as the LSM in the continuous phase with a 40/40/20 ratio when a formulation is loaded with 55 w/w% glass, 2.5 w/w% fumed silica, and 5 w/w% microcapsules. In Figure 4 (a) the sample 4D: TU was found to be a statistically lower flexural strength than all other samples in that figure. This shows that the lowest flexural strength occurs with TU as the LSM in the continuous phase with a 40/40/20 ratio when a formulation is loaded with 55 w/w% glass, 3.0 w/w% fumed silica, and 5 w/w% microcapsules. In Figure 5 (a) the samples 5D: TU 30/50/20 and 7D: TU 40/40/20 were found to have a statistically lower flexural strength than all other samples in that figure but not statistically different from each other. This shows that the lowest flexural strength occurs with TU as the LSM in the continuous phase with a 40/40/20 or 30/50/20 ratio when a formulation is loaded with 60 w/w% glass, 2.5 w/w% fumed silica, and 5 w/w% microcapsules.

From the trends found in Figures 3-7, the type of low stress monomer has an effect on the flexural strength of the sample. The Terethanes were not found to be statistically different from one another. The thiourethane oligomer consistently had a statistically lower flexural strength than all of the Terathanes.

In Figure 3 (b) the sample 2C: 650 Acr 40/40/20 was found to have a statistically greater fracture toughness than all other samples in that figure. The sample 1B: 1000 Meth 30/50/20 was the only other sample found to be statistically different with a lower fracture

toughness than samples 2C: 650 Acr 40/40/20 and 3D: TU 40/40/20. This illustrates that the greatest fracture toughness is achieved with 650 Acr as the LSM in the continuous phase with a 40/40/20 ratio while a lower fracture toughness is attained with 1000 Meth as the LSM in the continuous phase with a 30/50/20 ratio when a formulation is loaded with 55 w/w% glass, 2.5 w/w% fumed silica, and 5 w/w% microcapsules. In Figure 5 (b) the sample 7D: TU 40/40/20 was found to have a statistically greater fracture toughness than all other samples in that figure except 5D: TU 30/50/20. This illustrates that the greatest fracture toughness is achieved with TU as the LSM in the continuous phase with a 40/40/20 ratio when a formulation is loaded with 60 w/w% glass, 2.5 w/w% fumed silica, and 5 w/w% microcapsules. In Figure 6 (b) the samples 6D: TU 30/50/20 and 8D: TU 40/40/20 were found to be a statistically greater fracture toughness than the other sample in that figure but not statistically different from each other. This shows that the greatest fracture toughness occurs with TU as the LSM in the continuous phase with a 40/40/20 or 30/50/20 ratio when a formulation is loaded with 60 w/w% glass, 3.0 w/w% fumed silica, and 5 w/w% microcapsules.

From the trends found in Figures 3-7, the type of low stress monomer has an effect on the fracture toughness of the sample. The 650 Meth and 1000 Meth were not found to have statistically different fracture toughness from one another. In some cases, 650 Acr had a statistically greater fracture toughness than other Terathanes. The thiourethane oligomer consistently had a statistically higher than most of the Terathanes. This may be due to the fact that polymer network containing the thiourethane oligomer will have a more homogenous network than simple urethanes [60]. The use of a thiourethane oligomer increases the degree of conversion and reduces the rate of polymerization [61]. These

factors are thought to decrease the internal stress of the composite, which should increase its mechanical properties.

4.2.3 Constant LSM with different glass and fumed silica loading

Figures 8-11 illustrate the effect of loading a formulation with different amounts of glass or fumed silica while keeping the type and amount of low stress monomer within the continuous phase consistent. The hypothesis for these figures was that changing the amount of glass or fumed silica would change the flexural strength or fracture toughness of the sample. The null hypothesis is that the change in glass or fumed silica will have no effect on the flexural strength or fracture toughness.

In Figure 8 (a) the sample 5A: 63% glass, 2.5% FS 30/50/20 was found to have a statistically greater flexural strength than all other samples in that figure except 4A: 60% glass, 2.5% FS 30/50/20. This shows that the greatest flexural strength occurs when the formulation has the greatest amount of glass if 650 Meth is the LSM in the continuous phase.

From the trends found in Figures 8-11, the glass can have an effect on the flexural strength of the sample. For 650 Meth, when the glass loading increased the flexural strength also increased. For 1000 Meth and TU, there were statistical differences between the samples without a clear trend. For 650 Acr, most of the samples were not found to be statistically different from one another.

In Figure 8 (b) the sample 3A: 55% glass, 3.0% FS 40/40/20 was found to have a statistically lower fracture toughness than most other samples in that figure. This illustrates that the lowest fracture toughness occurs when the fumed silica is increased to 3.0 w/w% if 650 Meth is the LSM. In Figure 9 (b) the sample 4B: 60% glass, 3.0% FS 30/50/20 was

found to have a statistically lower fracture toughness than all other samples in that figure. This illustrates that the lowest fracture toughness occurs when the fumed silica is increased to 3.0 w/w% if 1000 Meth is the LSM. In Figure 10 (b) the sample 3C: 55% glass, 3.0% FS 40/40/20 was found to have a statistically lower fracture toughness than all other samples in that figure. This illustrates that the lowest fracture toughness occurs when the fumed silica is increased to 3.0 w/w% if 650 Acr is the LSM.

From the trends found in Figures 8-11, the fumed silica can have an effect on the fracture toughness of the sample. For Terathanes, when the fumed silica loading increased to 3.0 w/w% the fracture toughness decreased. For TU, there were statistical differences between the samples without a clear trend. As the loading of the small filler particles and total surface area of those particles requiring silane during the silanization process increases. The increased surface area where the filler meets the continuous phase may lead to an increased chance of interfacial failure [62].

4.3 Low viscosity monomer

4.3.1 Varied low stress monomer

Figures 12-14 show the effects of HEMA and HPMA on flexural strength and fracture toughness for the different low stress monomers. Figures 15-17 illustrate the effect on flexural strength and fracture toughness by adding 1 w/w% 10-MDP to the total mass of formulations with different low stress monomers. The hypothesis for these figures was that when the low stress monomer is changed in formulas containing a LVM the flexural strength or fracture toughness also changed. The null hypothesis is that the change in low stress monomer will have no effect on the flexural strength or fracture toughness in formulas containing a LVM.

From the trends found in Figures 12-17, the LSM can have an effect on the flexural strength of the sample. For Terathanes, when HEMA or HPMA is used as a LVM there were statistical differences between some of the samples without a clear trend. For each LSM, when 10-MDP is used as a LVM there were statistical differences between some of the samples without a clear trend.

In Figure 12 (b) the samples 7E: 1000 Meth, HEMA, 63% glass, 40/38/20/2 and 8E: 1000 Meth, HPMA, 63% glass, 40/38/20/2 were found to have a statistically lower fracture toughness than most other samples in that figure. This illustrates that the lowest fracture toughness occurs when 1000 Meth is used in the continuous phase with a ratio of 40/38/20/2 if HEMA or HPMA is used as a LVM. In figure 16 (b) the samples 5F: TU 30/50/20 and 9F: TU 40/40/20 were found to have a statistically greater fracture toughness than all other samples in that figure. This shows that the greatest fracture toughness occurs when TU is used as the LSM in the continuous phase with a 40/40/20 or 30/50/20 ratio when a formulation is loaded with 60 w/w% glass, 2.5 w/w% fumed silica, 5 w/w% microcapsules, and 1 w/w% 10-MDP in the total mass of the formulation. In Figure 17 (b) the sample 13F: TU was found to have a statistically greater fracture toughness than all other samples in that figure. This shows that the greatest fracture toughness occurs when TU is used as the LSM in the continuous phase with a 40/40/20 ratio when a formulation is loaded with 60 w/w% glass, 3.0 w/w% fumed silica, 5 w/w% microcapsules, and 1 w/w% 10-MDP in the total mass of the formulation.

From the trends found in Figures 12-17, the LSM can have an effect on the fracture toughness of the sample. For Terathanes, when HEMA, HPMA, or 10-MDP is used as a LVM there were statistical differences between some of the samples without a clear trend.

For the thiourethane oligomer, when 10-MDP is used as a LVM and the fumed silica is 2.5 w/w% or 3.0 w/w% the fracture toughness is greater than the other samples.

4.3.2 Low viscosity monomers

Figures 18-20 display the effect of 2, 5, and 10 w/w% HEMA or HPMA on flexural strength and fracture toughness when the type and amount of low stress monomer within the continuous phase is constant. The hypothesis for these figures was that when the type or amount of LVM is changed the flexural strength or fracture toughness of the sample also changed. The null hypothesis is that changing the type or amount of LVM will have no effect on the flexural strength or fracture toughness of the sample.

From the trends found in Figures 18-20, the type and amount of LVM can have an effect on the flexural strength of the sample. For 650 Meth, when the amount of HEMA or HPMA changed there was no statistical difference between any of the samples. For 1000 Meth and 650 Acr, when the amount of HEMA or HPMA changed there were statistical differences between some of the samples without a clear trend.

From the trends found in Figures 18-20, the type and amount of LVM can have an effect on the fracture toughness of the sample. For 650 Meth and 650 Acr, when the amount of HEMA or HPMA changed there were statistical differences between some of the samples without a clear trend. For 1000 Meth, when the amount of HEMA or HPMA was 5 or 10 w/w% in the continuous phase the fracture toughness was usually statistically greater than when HEMA or HPMA was 2 w/w% in the continuous phase.

4.3.3 Fumed silica

Figures 21-24 compare the effect of fumed silica on flexural strength and fracture toughness for the different low stress monomers when 10-MDP was used as a LVM. The hypothesis for these figures was that when the amount of fumed silica is changed the flexural strength or fracture toughness of the sample also changed. The null hypothesis is that changing the amount of fumed silica will have no effect on the flexural strength or fracture toughness of the sample.

In Figure 22 (a) the sample 3F: 2.0% FS 40/40/20 was found to have a statistically greater flexural strength than most other samples in that figure except 7F: 2.5% FS 30/50/20. This shows that the greatest flexural strength occurs when the formulation has the lowest amount of fumed silica if 1000 Meth is the LSM in the continuous phase and contains 1 w/w% 10-MDP in the total formulation. In Figure 24 (a) the sample 13F: 3.0% FS 40/40/20 was found to have a statistically lower flexural strength than most other samples in that figure except 9F: 2.5% FS 40/40/20. This shows that the lowest flexural strength occurs when the formulation has the greatest amount of fumed silica if TU is the LSM in the continuous phase and contains 1 w/w% 10-MDP in the total formulation.

From the trends found in Figures 21-24, the amount of fumed silica can have an effect on the flexural strength of the sample. For 650 Meth and 650 Acr, when the amount of fumed silica changed there were statistical differences between some of the samples without a clear trend. For 1000 Meth and TU, when the amount of fumed silica increased the flexural strength decreased.

In Figure 22 (b) the sample 3F: 2.0% FS 40/40/20 was found to have a statistically greater fracture toughness than all other samples in that figure. This shows

that the greatest fracture toughness occurs when the formulation has the lowest amount of fumed silica if 1000 Meth is the LSM in the continuous phase and contains 1 w/w% 10-MDP in the total formulation. In Figure 23 (b) the sample 4F: 2.0% FS 40/40/20 was found to have a statistically greater fracture toughness than all other samples in that figure. This shows that the greatest fracture toughness occurs when the formulation has the lowest amount of fumed silica if 650 Acr is the LSM in the continuous phase and contains 1 w/w% 10-MDP in the total formulation.

From the trends found in Figures 21-24, the amount of fumed silica can have an effect on the fracture toughness of the sample. For 650 Meth and TU, when the amount of fumed silica changed there were statistical differences between some of the samples without a clear trend. For 1000 Meth and 650 Acr, when the amount of fumed silica decreased to 2.0 w/w% the fracture toughness increased. Similar to the trend found in Figures 8-11, decreasing the load of the small filler will decrease the surface area coated with silane during the silanization process and the chance of interfacial failure [62].

4.4 Conclusion

In summary, every null hypothesis was rejected because each of the variables was shown to affect the flexural strength and fracture toughness. The affect that these variables caused did not always follow a clear trend. From these figures, two steady trends did emerge for flexural strength and fracture toughness. The flexural strength of a sample was consistently higher when the fumed silica load was lower and the sample contained a Terathane rather than the thiourethane oligomer. The fracture toughness was regularly higher when the fumed silica load was lower and the sample contained the thiourethane oligomer rather than a Terathane. The butoxy repeat units that make up a significant

amount of the molecular weight of the Terathanes provides rotational freedom that may have led to an increased flexural strength for the samples containing Terathanes over those with the thiourethane oligomer. The thiol functional groups found on the thiourethane oligomer work as a chain transfer agent, reducing the rate of polymerization of methacrylates [38-41] The resulting decrease in stress may be the cause for greater fracture toughness in samples containing the thiourethane oligomer over those containing Terathanes. The potential for developing a low stress, BPA free, ion eluting flowable composite/ base liner is promising. Future studies would have to be specifically designed to test further hypotheses as to why these specific formulations performed statistically better than others.

References

1. Higham S [webpage on the Internet] Caries Process and Prevention Strategies: Demineralization/Remineralization. [Accessed Jan 23, 2019]. Available from: <http://www.dentalcare.com/media/en-US/education/ce372/ce372.pdf>
2. West N.X., Joiner A. Enamel mineral loss. *J. Dent.* 2014;42:S2–S11. doi: 10.1016/S0300-5712(14)50002-4.
3. Cummins D. The development and validation of a new technology, based upon 1.5% arginine, an insoluble calcium compound and fluoride, for everyday use in the prevention and treatment of dental caries. *J Dent.* 2013;41(2):S1–S11.
4. Kleinberg I. A new saliva-based anti-caries composition. *Dent Today.* 1999;18(2):98–103.
5. Almeida e Silve JS, Baratieri L, Araujo E, Widmer N. Dental erosion: understanding this pervasive condition. *J Esthet Restor Dent.* 2011;23(4):205–216.
6. Tahmassebi JF, Duggal MS, Malik-Kotru G, Curzon MEJ. Soft drinks and dental health: a review of the current literature. *J Dent.* 2006;34(1):2–11.
7. Dowd F. Saliva and dental caries. *Dent Clin North Am.* 1999;43(4):579–597.
8. Arnold, W. H., Haase, A., Hacklaender, J., Gintner, Z., Bánóczy, J., & Gaengler, P. (2007). Effect of pH of amine fluoride containing toothpastes on enamel remineralization in vitro. *BMC Oral Health*, 7(1), 14.
9. Soncini JA, Maserejian NN, Trachtenberg F *et al.* The longevity of amalgam versus compomer/composite restorations in posterior primary and permanent teeth: findings From the New England Children's Amalgam Trial. *J Am Dent Assoc* 2007; 138: 763–772.
10. Kuper, N. K., Van De Sande, F. H., Opdam, N. J. M., Bronkhorst, E. M., De Soet, J. J., Cenci, M. S., & Huysmans, M. C. D. J. N. M. (2015). Restoration materials and secondary caries using an in vitro biofilm model. *Journal of dental research*, 94(1), 62-68.
11. Ruschel, V. C., Martins, M. V., Bernardon, J. K., & Maia, H. P. (2018). Color Match Between Composite Resin and Tooth Remnant in Class IV Restorations: A Case Series. *Operative dentistry*, 43(5), 460-466.
12. Shouha, P., Swain, M., & Ellakwa, A. (2014). The effect of fiber aspect ratio and volume loading on the flexural properties of flowable dental composite. *Dental materials*, 30(11), 1234-1244.
13. Kopperud S.E., Tveit A.B., Gaarden T., Sandvik L., Espelid I. Longevity of posterior dental restorations and reasons for failure. *Eur. J. Oral Sci.* 2012;120:539–548. doi: 10.1111/eos.12004.
14. Silvani S., Trivelato R.F., Nogueira R.D., de Souza Gonçalves L., Geraldo-Martins V.R. Factors affecting the placement or replacement of direct restorations in a dental school. *Contemp. Clin. Dent.* 2014;5:54–58.

15. Van Dijken J.W., Pallesen U. A six-year prospective randomized study of a nano-hybrid and a conventional hybrid resin composite in Class II restorations. *Dent Mater*. 2013;29:191–198. doi: 10.1016/j.dental.2012.08.013.
16. Pallesen U, van Dijken JW. A randomized controlled 30 years follow up of three conventional resin composites in Class II restorations. *Dent Mater* 2015;31:1232–44.
17. Beck F, Lettner S, Graf A, Bitriol B, Dumitrescu N, Bauer P, et al. Survival of direct resin restorations in posterior teeth within a 19-year period (1996-2015): a meta-analysis of prospective studies. *Dent Mater* 2015;31:958–85.
18. Ástvaldsdóttir Á, Dagerhamn J, van Dijken JW, Naimi-Akbar A, Sandborgh-Englund G, Tranæus S, et al. Longevity of posterior resin composite restorations in adults — a systematic review. *J Dent* 2015;43:934–54.
19. MJÖR, I. A. (2005). Clinical diagnosis of recurrent caries. *The Journal of the American Dental Association*, 136(10), 1426-1433.
20. Kleverlaan, C. J., & Feilzer, A. J. (2005). Polymerization shrinkage and contraction stress of dental resin composites. *Dental Materials*, 21(12), 1150-1157.
21. Yamasaki, L. C., Moraes, A. G. D. V., Barros, M., Lewis, S., Francci, C., Stansbury, J. W., & Pfeifer, C. S. (2013). Polymerization development of “low-shrink” resin composites: Reaction kinetics, polymerization stress and quality of network. *Dental Materials*, 29(9), e169-e179.
22. Dauvillier BS, Aarnts MP, Feilzer AJ. Developments in shrinkage control of adhesive restoratives. *Journal of Esthetic Dentistry* 2000;12(6):291–9.
23. Gerdolle DA, Mortier E, Droz D. Microleakage and polymerization shrinkage of various polymer restorative materials. *Journal of Dentistry for Children (Chicago)* 2008;75(2):125–33.
24. Brunthaler A, König F, Lucas T, Sperr W, Schedle A. Longevity of direct resin composite restorations in posterior teeth. *Clinical Oral Investigations* 2003;7(2):63–70.
25. Feilzer AJ, De Gee AJ, Davidson CL. Curing contraction of composites and glass-ionomer cements. *Journal of Prosthetic Dentistry* 1988;59(3):297–300.
26. Borkowski K, Kotousov A, Kahler B. Effect of material properties of composite restoration on the strength of the restoration–dentine interface due to polymerization shrinkage, thermal and occlusal loading. *Medical Engineering and Physics* 2007;29(6):671–6.
27. Pereira RA, Araujo PA, Castaneda-Espinosa JC, Mondelli RF. Comparative analysis of the shrinkage stress of composite resins. *Journal of Applied Oral Science* 2008;16(1):30–4.
28. Boaro LC, Fróes-Salgado NR, Gajewski VE, Bicalho AA, Valdivia AD, Soares CJ, et al. Correlation between polymerization stress and interfacial integrity of

- composites restorations assessed by different in vitro tests. *Dent Mater* 2014;30:984–92.
29. Ferracane JL, Hilton TJ. Polymerization stress — is it clinically meaningful? *Dent Mater* 2016;32:1–10.
 30. Soares CJ, Faria-E-Silva AL, Rodrigues MP, Vilela ABF, Pfeifer CS, Tantbirojn D, et al. Polymerization shrinkage stress of composite resins and resin cements — what do we need to know? *Braz Oral Res* 2017;31:e62.
 31. Bicalho AA, Valdívia AD, Barreto BC, Tantbirojn D, Versluis A, Soares CJ. Incremental filling technique and composite material — part II: shrinkage and shrinkage stresses. *Oper Dent* 2014;39:E83–92.
 32. Dewaele M, Truffier-Boutry D, Devaux J, Leloup G. Volume contraction in photocured dental resins: the shrinkage–conversion relationship revisited. *Dental Materials* 2006;22(4):359–65.
 33. Atai M, Watts DC, Atai Z. Shrinkage strain-rates of dental resin-monomer and composite systems. *Biomaterials* 2005; 26:5015-5020.
 34. Condon JR, Ferracane JL. Assessing the effect of composite formulation on polymerization stress. *Journal of the American Dental Association* 2000;131(4):497–503.
 35. Labella R, Lambrechts P, Van Meerbeek B, Vanherle G. Polymerization shrinkage and elasticity of flowable composites and filled adhesives. *Dental Materials* 1999;15(2):128–37.
 36. Moraes RR, Garcia JW, Barros MD, Lewis SH, Pfeifer CS, Liu J, et al. Control of polymerization shrinkage and stress in nanogel-modified monomer and composite materials. *Dent Mater* 2011;27:509–19.
 37. Maghaireh GA, Taha NA, Alzraikat H. The silorane-based resin composites: a review. *Oper Dent* 2017;42:E24–34.
 38. Lu H, Carioscia JA, Stansbury JW, Bowman CN. Investigations of step-growth thiol-ene polymerizations for novel dental restoratives. *Dent Mater* 2005;21:1129–36.
 39. Park HY, Kloxin CJ, Scott TF, Bowman CN. Stress relaxation by addition-fragmentation chain transfer in highly crosslinked thiol-yne networks. *Macromolecules* 2010;43:10188–90.
 40. Bacchi A, Pfeifer CS. Rheological and mechanical properties and interfacial stress development of composite cements modified with thio-urethane oligomers. *Dent Mater* 2016;32:978–86.
 41. Bacchi A, Nelson M, Pfeifer CS. Characterization of methacrylate-based composites containing thio-urethane oligomers. *Dent Mater* 2016;32:233–9.

42. Liliana, R., Slawomir, G., Tomasz, J., Joanna, W., & Andrzej, P. (2019). The effects of Bisphenol A (BPA) on sympathetic nerve fibers in the uterine wall of the domestic pig. *Reproductive Toxicology*, 84, 39-48.
43. Maserejian, N. N., Trachtenberg, F. L., Wheaton, O. B., Calafat, A. M., Ranganathan, G., Kim, H. Y., & Hauser, R. (2016). Changes in urinary bisphenol A concentrations associated with placement of dental composite restorations in children and adolescents. *The Journal of the American Dental Association*, 147(8), 620-630.
44. Y. Hu, S. Wen, D. Yuan, L. Peng, R. Zeng, Z. Yang, Q. Liu, L. Xu, D. Kang, The association between the environmental endocrine disruptor bisphenol A and polycystic ovary syndrome: a systematic review and meta-analysis, *Gynecol. Endocrinol.* 34 (2018) 370–377.
45. L.C. Ge, Z.J. Chen, H.Y. Liu, K.S. Zhang, H. Liu, H.B. Huang, G. Zhang, C.K. Wong, J.P. Giesy, J. Du, H.S. Wang, Involvement of activating ERK1/2 through G protein coupled receptor 30 and estrogen receptor α/β in low doses of bisphenol A promoting growth of Sertoli TM4 cells, *Toxicol. Lett.* 226 (2014) 81–89.
46. D. Nesan, L.C. Sewell, D.M. Kurrasch, Opening the black box of endocrine disruption of brain development: lessons from the characterization of Bisphenol A, *Horm. Behav.* 101 (2018) 50–58, <https://doi.org/10.1016/j.yhbeh.2017.12.001>.
47. Testai, E., Hartemann, P., Rodríguez-Farré, E., Rastogi, S. C., de Jong, W., Bustos, J., ... & Olea, N. (2015). The safety of the use of bisphenol A in medical devices. <http://dx.doi.org/10.2772/75546>, 18 February, ISBN 978-92-79-30133-9.
48. Ku, H. S., Fok, S. C., & Siores, E. (2009). Contrasts on fracture toughness and flexural strength of varying percentages of SLG-reinforced phenolic composites. *Journal of composite materials*, 43(8), 885-895.
49. Janda, R., Roulet, J. F., & Latta, M. (2006). The effects of thermocycling on the flexural strength and flexural modulus of modern resin-based filling materials. *Dental Materials*, 22(12), 1103-1108.
50. Falbo, M. (2012) The release of calcium, fluoride, and phosphate ions from ion permeable microcapsules in a rosin varnish. Published dissertation. Creighton University.
51. Fulton, J (2013) The Effect of Continuous Phase and Glass Content on Fracture toughness and Calcium and Phosphate Ion Release from Ion Permeable Microcapsules in Glaze Formulations Published dissertation. Creighton University
52. Cooper, R. (2013) Encapsulation of Calcium and Phosphate Ions in a Toothpaste Formulation, Published dissertation. Creighton University
53. Adler, E. R. (2017). Flexural Strength of Orthodontic Cement Containing Microcapsules, Published dissertation. Creighton University

54. Jun, S. K., Kim, H. W., Lee, H. H., & Lee, J. H. (2018). Zirconia-incorporated zinc oxide eugenol has improved mechanical properties and cytocompatibility with human dental pulp stem cells. *Dental Materials*, 34(1), 132-142.
55. Ilie, N., Hickel, R., Valceanu, A. S., & Huth, K. C. (2012). Fracture toughness of dental restorative materials. *Clinical Oral Investigations*, 16(2), 489-498.
56. Bacchi, A., Nelson, M., & Pfeifer, C. S. (2016). Characterization of methacrylate-based composites containing thio-urethane oligomers. *Dental Materials*, 32(2), 233-239.
57. Dobson, A., Bacchi, A., & Pfeifer, C. S. (2014). Thio-urethane oligomers reduce polymerization stress in highly filled dental composites. *Dental Materials*, (30), e75.
58. Hambire, U., Tripathi, V., & Mapari, A. (2012). Improvement in the compressive strength and flexural strength of dental composite. *ARPJ Eng Appl Scie*, 7(8), 1-4.
59. Asmussen, E., & Peutzfeldt, A. (1998). Influence of UEDMA, BisGMA and TEGDMA on selected mechanical properties of experimental resin composites. *Dental Materials*, 14(1), 51-56.
60. Senyurt AF, Hoyle CE. Thermal and mechanical properties of cross-linked photopolymers based on multifunctional thiol-urethane ene monomers. *Macromolecules* 2007;40:3174–82.
61. Bacchi, A., Consani, R. L., Martim, G. C., & Pfeifer, C. S. (2015). Thio-urethane oligomers improve the properties of light-cured resin cements. *Dental Materials*, 31(5), 565-574.
62. Junior, R., Adalberto, S., Zanchi, C. H., Carvalho, R. V. D., & Demarco, F. F. (2007). Flexural strength and modulus of elasticity of different types of resin-based composites. *Brazilian oral research*, 21(1), 16-21.